arXiv:2504.11216v1 [cs.LG] 15 Apr 2025

Diversity-Driven Learning: Tackling Spurious Correlations and Data Heterogeneity in Federated Models

Gergely D. Németh *gergely@ellisalicante.org*
ELLIS Alicante

Eros Fanì
Polytechnic Institute of Turin
Basque Center for Applied Mathematics

Yeat Jeng Ng
University of Sussex

Barbara Caputo
Polytechnic Institute of Turin
Sapienza University of Rome

Miguel Ángel Lozano
University of Alicante

Nuria Oliver
ELLIS Alicante

Novi Quadrianto
University of Sussex
Basque Center for Applied Mathematics
Monash Indonesia

Abstract

Federated Learning (FL) enables decentralized training of machine learning models on distributed data while preserving privacy. However, in real-world FL settings, client data is often non-identically distributed and imbalanced, resulting in statistical data heterogeneity which impacts the generalization capabilities of the server's model across clients, slows convergence and reduces performance. In this paper, we address this challenge by first proposing a characterization of statistical data heterogeneity by means of 6 metrics of global and client attribute imbalance, class imbalance, and spurious correlations. Next, we create and share 7 computer vision datasets for binary and multiclass image classification tasks in Federated Learning that cover a broad range of statistical data heterogeneity and hence simulate real-world situations. Finally, we propose FedDiverse, a novel client selection algorithm in FL which is designed to manage and leverage data heterogeneity across clients by promoting collaboration between clients with complementary data distributions. Experiments on the seven proposed FL datasets demonstrate FedDiverse's effectiveness in enhancing the performance and robustness of a variety of FL methods while having low communication and computational overhead.

1 Introduction

In centralized machine learning, all training data is shared with a central server, posing privacy, regulatory, and ethical concerns, especially for sensitive data [LSTS20]. Federated learning (FL) [MMR+17] aims to address these concerns by enabling decentralized, privacy-preserving model training without transferring raw

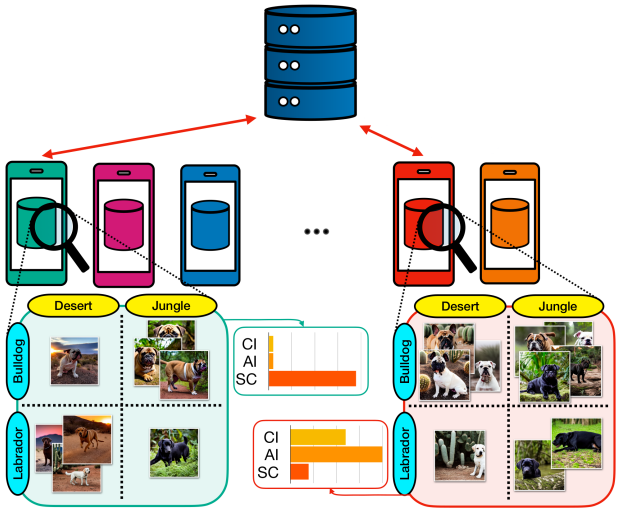

Figure 1: Visual representation of FedDiverse. CI, AI, and SC stand for Class Imbalance, Attribute Imbalance, and Spurious Correlation in the clients' data distributions. Observe the statistical data heterogeneity in the selected clients (turquoise and red). FedDiverse automatically selects clients with a diversity of local statistics to learn a global model that is resilient to statistical data heterogeneity.

data. In FL, models are trained collaboratively across distributed *clients*. Each training round consists of: (1) the server sharing the global model with selected clients, (2) clients performing local training, and (3) clients sending updated model parameters back to the server for aggregation. This decentralized process maintains data privacy while improving the global model.

In real-world FL scenarios, client data is often shaped by local factors such as differing user behaviors [TYCY22], context-specific data collection environments [FMO20; YAE+18], and socio-economic or cultural biases [BCM+18], resulting in *statistical data heterogeneity*, where data across different clients is non-independent and identically distributed (non-IID) and imbalanced. Statistical data heterogeneity hampers the generalization capabilities of the server's model across clients, slowing convergence and reducing performance [LHY+20; CCC22].

Previous studies in FL have addressed statistical data heterogeneity from an algorithmic perspective, providing convergence theorems, analyzing computational costs, and proposing solutions to mitigate its effects [KKM+20; LHY+20; AZM+21; LSTS20]. However, there is a lack of fine-grained analyses of this problem. In this paper, we address this gap and propose decomposing the *attribute-target label* relationships to identify three types of statistical data heterogeneity: (1) *class imbalance* (CI), when target labels have asymmetric distributions; (2) *attribute imbalance* (AI), when attributes exhibit imbalanced distributions; and (3) *spurious correlations* (SC), that emerge when the model learns misleading correlations between a non-discriminative attribute, such as the background, and the target label. These three types of data heterogeneity pose a challenge both in centralized [YLCT20; YZKG23] and federated [KMA+21; MBB24] learning.

Prior work in centralized machine learning has shown that CI, AI, and SC often arise when data is limited or lacks sufficient diversity [YZC+24; GJM+20]. Thus, a typical solution consists of using an additional and diverse yet unlabeled dataset –called "validation", "target" or "deployment" dataset– to do self-training (*e.g.* [LHC+21; CWKM20]) or to learn a representation that is invariant to attributes (*e.g.* [TCK+21]).

In FL, the *diversity* of client data can be leveraged to devise client selection methods that mitigate the effects of CI, AI, and SC. By prioritizing clients with complementary data distributions, the server's model is exposed to diverse training patterns without accessing raw data, enhancing generalization while preserving privacy.

In this paper, we leverage this idea and address the challenge of statistical data heterogeneity in FL by proposing a novel client selection algorithm called FedDiverse that takes advantage of diversity in client data distributions. We empirically evaluate FedDiverse on 7 computer vision datasets that exhibit varying levels of CI, AI and SC, leading to the following **contributions**:

(1) We propose a fine-grained analysis of statistical data heterogeneity in FL by means of 6 metrics;

(2) We introduce and share 7 FL datasets for binary and multiclass image classification tasks that cover a broad range statistical data heterogeneity;

(3) We present FedDiverse, illustrated in Fig. 1, a novel client selection method that is designed to mitigate the impact of statistical data heterogeneity (CI, AI and SC) in FL training while ensuring the privacy of clients and respecting the resource-constrained nature of each client.

2 Related Work

2.1 Data Heterogeneity in Federated Learning

Statistical heterogeneity or non-IID data is a major concern in FL because it can hinder the training process, leading to poor generalization and slow and unstable convergence [KMA+21]. Various methods have been proposed to address this issue [MBB24]. Some approaches add regularization terms to align local updates with the global model, such as FedDyn [AZM+21] and FedProx [LSTS20], while other methods aim to reduce variance between client updates, such as SCAFFOLD [KKM+20], MOON [LHS21], and FedFM [YNX+23]. In other approaches, the clients share additional information with the server that reveals information about their statistical data heterogeneity. In pow-d [CWJ22], clients share the average loss of the previous global model applied to their local data; in IGPE [ZWL+24] they share averaged network embeddings; and in FedAF [WFK+24] they share synthetic data. Finally, optimization-based server-side methods, such as FedAvgM [HQB19], MIME [KJK+20], and FedOpt [RCZ+20], employ adaptive learning rates at the server to manage statistical diversity among clients.

However, none of these strategies explicitly addresses the challenge posed by spurious correlations in client data, leaving room for improvement.

2.2 Spurious Correlations in Centralized ML

Spurious correlations can significantly hinder robustness and generalization in machine learning [YZC+24; GJM+20; NAN20]. Proposed solutions to this problem fall into two main categories. The first category [SKHL20; ABGL19; YWL+22] unrealistically assumes that spurious attributes are known or partially labeled, enabling models to reduce reliance on these attributes by re-weighting samples or modifying training processes. These methods often require that data groups or environments be explicitly defined to minimize spurious dependencies.

The second category does not assume prior knowledge of spurious attributes. Instead, models are designed to automatically distinguish meaningful patterns from spurious ones, often using techniques such as adversarial training [KKK+19; CYZ19] or counterfactual data augmentation [KHL19; WZY+19]. For example, LfF trains two models concurrently: a biased model to capture dataset biases and a debiased one trained on reweighted samples influenced by the biased model's predictions [NCA+20]; and Just-Train-Twice initially identifies "failure" cases where the model misclassifies, then increases the weights of these cases in a second training phase to improve robustness against spurious features [LHC+21].

Even though spurious correlations have been sparsely studied in the FL literature, recent research has begun to explore this challenge. To the best of our knowledge, [WZNK24] is the first piece of work to tackle spurious correlations in FL by investigating personalization such that models are tailored to the individual clients' data. In contrast, we aim to learn a single global model that remains robust to spurious correlations across all client distributions, achieving strong generalization performance for all clients.

2.3 Client Selection and Weighting in FL

Client selection and client weighting are two primary strategies in FL to manage client contributions during training and mitigate the challenges posed by heterogeneous data [NLQO22]. In client selection, which is especially relevant in resource-constrained settings, only a subset of clients participate in each training round to reduce communication and resource demands, improving training efficiency. Conversely, client weighting includes all clients in each round but adjusts their influence on the global model by means of a weight, aiming to accelerate convergence and performance [CGSY18; DLS21; CWJ22]. Both strategies support fairness [ZFH21; CKMT18] and security [RMLH22; BEGS17], mitigating effects from clients with unreliable or adversarial data.

Client selection or client weighting strategies address the challenge of statistical heterogeneity in FL by prioritizing or scaling the client contributions based on data quality and relevance. In the client selection category, methods like FedPNS [WW22] and pow-d [CWJ22] prioritize clients that are expected to contribute significantly to model accuracy, either through gradient similarity to the average model gradient or by selecting clients whose data produces high loss on the server's model. Fed-CBS aims to reduce the class-imbalance by selecting the clients that will generate a more class-balanced grouped dataset [ZLT+23].

Client clustering is a common technique for selecting clients that represent groups that share similar data distributions[1]. Server-side clustering methods typically consider the similarity of the client gradient updates as a proxy of the similarity between their data distributions (e.g., FCCPS [XZLD22]) or their projection into a lower dimension for compression (e.g. HCSFed [SSG+23]). In addition, clients can send metrics that describe the statistical heterogeneity of their local data, such as entropy in HiCS-FL [CV25]. Sharing the full characteristics of the client data distribution with the server has also been investigated [PLY23; WSK+22], yet it could be considered a privacy violation [CV25], and it is typically unknown for spurious correlations. Finally, client weighting methods, such as CI-MR [STW19], FMore [ZZWC20] and FedNova [WLL+20], reward clients with high-value data or normalize updates to counter statistical heterogeneity.

Although most existing methods address non-IID data in FL through class imbalance, we study other types of statistical heterogeneity, such as attribute imbalance and spurious correlations, as described next.

3 A Framework of Data Heterogeneity in FL

3.1 Background and Problem Setup

Let $f : \mathcal{X} \to \mathcal{Y}$ be a predictor function parameterized by $\theta \in \Theta$, where $\mathcal{X}$ is the feature space, $\mathcal{Y}$ is the output space, and Θ is the parameter space. We assume that the feature space consists of two subspaces: $\mathcal{X} \subseteq \mathcal{X}_y \times \mathcal{X}_a$, where $\mathcal{X}_y$ and $\mathcal{X}_a$ represent the *task-intrinsic* and the *attribute* feature spaces, respectively. The class label $y \in \mathcal{Y}$ of a sample $x := (x_y, x_a)$ is determined by the discriminative feature x_y whereas the attribute label $a \in \mathcal{A}$ is determined by the attribute feature x_a, where $\mathcal{A}$ is the space of attributes. The training dataset D consists of n feature-target sample pairs[2], $D = \{(x_i, y_i)\}_{i=1}^n$, where each sample is identically and independently drawn from the training distribution $\mathbb{P}_{\text{tr}}$.

In a FL scenario, the dataset D composed of n samples is split across K clients $k \in \mathcal{K}$. In other words, each client k has access to a local, private dataset D_k such that $D = \bigcup_{k\in\mathcal{K}} D_k$, $|D_k| := n_k$, and $\sum_{k\in\mathcal{K}} n_k = n$, which cannot be accessed neither by the server $\mathcal{S}$ nor by any other client $j \neq k \in \mathcal{K}$. The FL objective is to find optimal parameters $\theta^* \in \Theta$ by solving the following problem:

$$\theta^* = \arg\min_{\theta\in\Theta} \sum_{k\in\mathcal{K}} \frac{n_k}{n} \mathcal{L}_k(\theta), \tag{1}$$

where $\mathcal{L}_k(\theta) = \sum_{(x,y)\in D_k} \ell(f(x;\theta), y)$ and ℓ is any loss function.

[1] We exclude works referred as clustered federated learning (FL), where each client cluster trains a separate model personalized to the data distribution of that cluster [GTL23; HSF+23], as our aim is to train one robust model shared by all clients.

[2] In this work, we assume that the labeling of the attribute is not available in the training set.

In practice, federated learning is orchestrated by a central server $\mathcal{S}$, which schedules the training into $T > 0$ rounds. During each round t, $0 < t \leq T$, a set $\mathcal{K}' \subseteq \mathcal{K}$ of clients is sampled by $\mathcal{S}$ and shares the current global parameters θ^t with them. Then, each client $k \in \mathcal{K}'$ initializes its local model with the received parameters and trains it using its local dataset D_k, obtaining new parameters θ_k^{t+1}. Finally, each sampled client shares its parameters with the server $\mathcal{S}$, where they are aggregated to form new global parameters θ^{t+1}. In the case of the standard FedAvg [MMR+17], this parameter aggregation is performed by computing the weighted mean: $\theta^{t+1} = \sum_{k \in \mathcal{K}'} \frac{n_k}{n} \theta_k^{t+1}$. This procedure is repeated for several rounds until convergence.

3.2 Statistical Data Heterogeneity

Statistical data heterogeneity emerges when there is a subpopulation shift, *i.e.*, when the representation of subpopulations differs between the training $\mathbb{P}_{tr}$ and the test $\mathbb{P}_{te}$ distributions. Here, subpopulations are defined by the target labels and the attributes, $\mathcal{Y} \times \mathcal{A}$. We consider three types of statistical data heterogeneity:

Class Imbalance (CI): The distribution of the target labels y is different between the training and test distributions, such that certain classes are more prevalent in the training than in the test sets, *i.e.*: $\mathbb{P}_{\text{tr}}(Y = y) \gg \mathbb{P}_{\text{tr}}(Y = y')$ for some $y, y' \in \mathcal{Y}$ where $y \neq y'$. CI can yield a biased classifier that performs poorly in samples from the minority class.

Attribute Imbalance (AI): The probability of occurrence of a certain attribute a' in the training set is much smaller than other attributes $a \in \mathcal{A}$ and this disparity in prevalence does not hold in the test distribution, *i.e.*, $\mathbb{P}_{\text{tr}}(A = a) \gg \mathbb{P}_{\text{tr}}(A = a')$. AI can yield a biased classifier towards the majority attribute a.

Spurious Correlation (SC): There is a statistical dependency between the class Y and the attribute A in the training distribution, which does not exist in the test distribution, *i.e.*, $\mathbb{P}_{\text{tr}}(Y = y \mid A = a) \gg \mathbb{P}_{\text{tr}}(Y = y) \gg \mathbb{P}_{\text{tr}}(Y = y \mid A = a')$, for some $y \in \mathcal{Y}$ and $a, a' \in \mathcal{A}$. This spurious dependency can cause a classifier to perform well on samples where the spurious relationship holds (*e.g.*, $(Y = y, A = a)$), but to underperform where the relationship does not hold (*e.g.*, $(Y = y, A = a')$).

3.3 Data Heterogeneity Metrics

Centralized Metrics. To measure the degree of statistical data heterogeneity in dataset D, we adopt the metrics proposed in [YZKG23]:

$$\Delta_{\text{CI}}(D) = 1 - H(Y)/\log|\mathcal{Y}| \tag{2}$$

$$\Delta_{\text{AI}}(D) = 1 - H(A)/\log|\mathcal{A}| \tag{3}$$

$$\Delta_{\text{SC}}(D) = 2I(Y;A)/(H(Y) + H(A)) \tag{4}$$

where H and I are the entropy and mutual information with respect to the empirical distribution of the dataset, respectively. Each metric is bounded within $[0, 1]$.

Federated Learning Metrics. We present six metrics –three global and three local– that characterize statistical data heterogeneity in FL, expanding the previously presented metrics for centralized learning.

Global FL metrics. In the FL context, when the metrics in Equations (2) to (4) are computed on the union of the clients' datasets, *i.e.* $D = \bigcup_{k \in \mathcal{K}} D_k$, they provide a global understanding of the severity of CI, AI and SC, namely:

$$\textbf{Global Class Imbalance: } GCI = \Delta_{\text{CI}}(D) \tag{5}$$

$$\textbf{Global Attribute Imbalance: } GAI = \Delta_{\text{AI}}(D) \tag{6}$$

$$\textbf{Global Spurious Correlation: } GSC = \Delta_{\text{SC}}(D) \tag{7}$$

Client FL metrics. The global FL metrics fail to capture the heterogeneity present in the datasets of individual clients. To this end, we propose three additional client metrics, where the local values of CI, AI

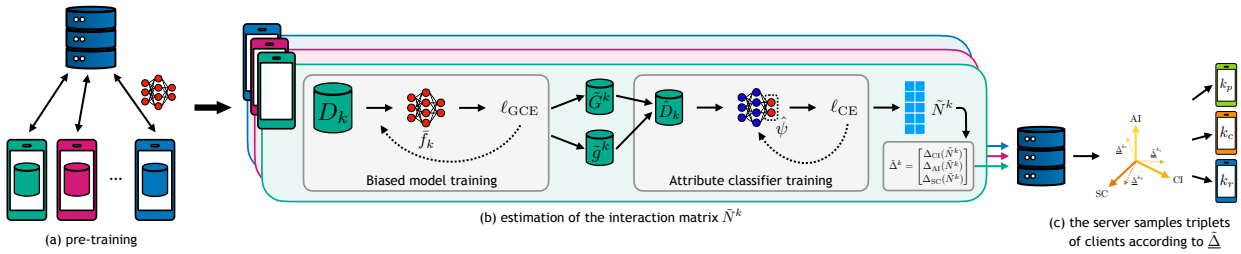

Figure 2: Main steps of FedDiverse. First (a), there is a phase of standard federated model pre-training. Second (b), the clients estimate their interaction matrices and, from them, their data heterogeneity triplets, which they share with the server. Finally, (c), the server uses the received triplets to perform client selection. Learnable parameters are marked in red, while fixed parameters are in blue.

and SC are averaged across all the K clients:

$$\textbf{Client Class Imbalance: } CCI = \frac{1}{K}\sum_{k\in\mathcal{K}} \Delta_{\text{CI}}(D_k) \tag{8}$$

$$\textbf{Client Attribute Imbalance: } CAI = \frac{1}{K}\sum_{k\in\mathcal{K}} \Delta_{\text{AI}}(D_k) \tag{9}$$

$$\textbf{Client Spurious Correlation: } CSC = \frac{1}{K}\sum_{k\in\mathcal{K}} \Delta_{\text{SC}}(D_k) \tag{10}$$

In practice, data heterogeneity often consists of a mixture of CI, AI and SC in the data distributions of different clients, as shown in Fig. 1 where Bulldog/Labrador is the target label and Desert/Jungle as the non-discriminative attribute in the image classification task.

4 Client Selection via FedDiverse

The proposed FedDiverse method consists of two components, illustrated in Fig. 2 and described next. First, an approach to estimate the statistical data heterogeneity in the clients, characterized by their local CI, AI and SC (Sec. 4.1). Second, a client selection strategy designed to include diverse clients in each round from the perspective of their statistical data heterogeneity (Sec. 4.2).

4.1 Estimation of the Statistical Data Heterogeneity

Preliminaries. The global *interaction matrix* N represents the count of samples in a global dataset D by class $\mathcal{Y}$ and attribute $\mathcal{A}$. For each client k, a local interaction matrix N^k captures its own non-normalized joint distribution of classes and attributes in their dataset D_k, such that $N = \sum_{k\in\mathcal{K}} N^k$. Although clients cannot access the full distribution of their interaction matrices due to unknown attribute distributions, each can compute a marginal interaction vector $M^k \in \mathbb{N}^{|Y|} : M^k_y = \sum_{a\in\mathcal{A}} N^k_{ya}$, where N^k_{ya} are the number of samples belonging to class $y \in Y$ and attribute $a \in A$ in the client's dataset D_k. Therefore, M^k_y contains the distribution of the classes in dataset D_k.

The interaction matrix reflects the precise, non-normalized distributions of classes and attributes. In cases with strong spurious correlations, local models may rely on an attribute a which is the most correlated with the class y instead of intrinsic class features. For each client, the *majority group* for a class y, denoted as G^k_y, includes the samples where the attribute a has the highest count in N^k, and the *minority group*, g^k_y, includes samples where a has the lowest count. By aggregating these for each class, we define the majority group for client k as G^k and the minority group as g^k. Because clients do not fully know the attribute function, they estimate these groups.

Finally, under the assumption that there are two attributes ($|\mathcal{A}| = 2$), the attribute set can be defined as $A = \{a_0, a_1\}$. This structure allows clients to infer the minority group attributes for a class y once they know the majority group attribute. Note that most datasets addressing SC or AI problems typically contain only two attributes (see Table 2 in [YZKG23]).

Estimation of the interaction matrices. Each client k approximates N^k as $\tilde{N}^k$ and uses this estimated matrix to compute its data heterogeneity triplet (DHT), $\tilde{\Delta}^k = [\Delta_{\text{CI}}(\tilde{N}^k), \Delta_{\text{AI}}(\tilde{N}^k), \Delta_{\text{SC}}(\tilde{N}^k)]^\top$[3]. To preserve privacy, the clients only share the triplet with the server, which uses these triplets to select clients, as explained in Section 4.2.

In the following, we outline the three-step method adopted by the clients to estimate their interaction matrices $\tilde{N}^k$ and hence their data heterogeneity triplets $\tilde{\Delta}^k$. Note that this estimation is only performed once at the beginning of the FL training process.

1. Pre-training: A global pre-training phase is carried out for a small number of rounds T_0 using the FedAvg algorithm, resulting in the global parameters θ^{T_0}.

2. Learning a Biased Model: After pre-training, each client receives θ^{T_0} and overfits a local model called a *biased model* $\bar{f}_k$ to its own data using the generalized cross-entropy loss function ℓ_{GCE} [ZS18]. This loss function encourages the model to rely more heavily on easy-to-learn patterns, which are often associated with spurious correlations [NCA+20]. As a result, each client can distinguish between a majority group G^k (where the majority of correctly predicted samples will belong) and a minority group g^k (where the incorrectly predicted samples will mainly belong). The predicted majority and minority groups for class y are denoted by $\tilde{G}^k_y$ and $\tilde{g}^k_y$, $\forall y \in \mathcal{Y}$, respectively. Given the nature of the ℓ_{GCE} loss, for $|\mathcal{Y}| > 2$, we train one-vs-rest binary classifiers $\bar{f}^y_k$ for each $y \in \mathcal{Y}$ to determine $\tilde{G}^k_y$ from the correctly predicted samples.

3. Attribute classifier: Using the biased model, clients label samples in the majority and minority groups, even though they lack information about the exact attribute labels. They identify a "pivot class" which has the smallest difference in sample size between the predicted majority and minority groups, *i.e.* $\hat{y} = \arg\min_{y \in \mathcal{Y}} \left| |\tilde{G}^k_y| - |\tilde{g}^k_y| \right|$. This class forms a new dataset $\hat{D}_k$, which contains all the samples in D_k whose class is $\hat{y}$. Each client then trains an *attribute classifier* $\hat{\psi}$ locally on $\hat{D}_k$ using cross-entropy loss to predict the attribute labels. This classifier yields an approximate interaction matrix $\tilde{N}^k$ by predicting the attributes according to the attribute labels in $\hat{D}_k$. Finally, each client computes their approximate DHT $\tilde{\Delta}^k$ and sends it to the server $\mathcal{S}$.

The server collects all the triplets sent by the clients in the *approximate data heterogeneity matrix* $\tilde{\Delta} \in [0,1]^{3 \times K}$ where each column corresponds to one client k and each row corresponds to the CI, AI, and SC components of the clients' $\tilde{\Delta}^k$.

Note that the final values of the scores in $\tilde{\Delta}^k$ are the same independently of the specific labeling choice for the $\hat{D}_k$ dataset, *i.e.* clients could equivalently assign the attribute label 1 to the majority group samples and 0 to the minority group samples. Moreover, sharing the $\tilde{\Delta}^k$ does not disclose private information from the clients and only incurs negligible additional communication costs. Thus, this approach is suitable for resource-constrained scenarios.

4.2 Client Selection

The rationale of FedDiverse is to sample clients with different types of statistical data heterogeneity (CI, AI and SC) in each round, leveraging it to achieve better generalization and robustness to real-word shifts [GTL23; ZLT+23; PLY23; HSF+23].

FedDiverse's client selection is achieved by leveraging the information in the triplet $\tilde{\Delta}^k$ received from each client and sampling clients to ensure diversity in the three dimensions of the triplets, *i.e.*, selecting clients whose datasets exhibit a variety of CI, AI and SC. The client selection consists of the following three steps.

[3] The metrics in Eqs. (2) to (4) can be equivalently calculated using the interaction matrix, as it fully describes the non-normalized joint distribution of classes and attributes.

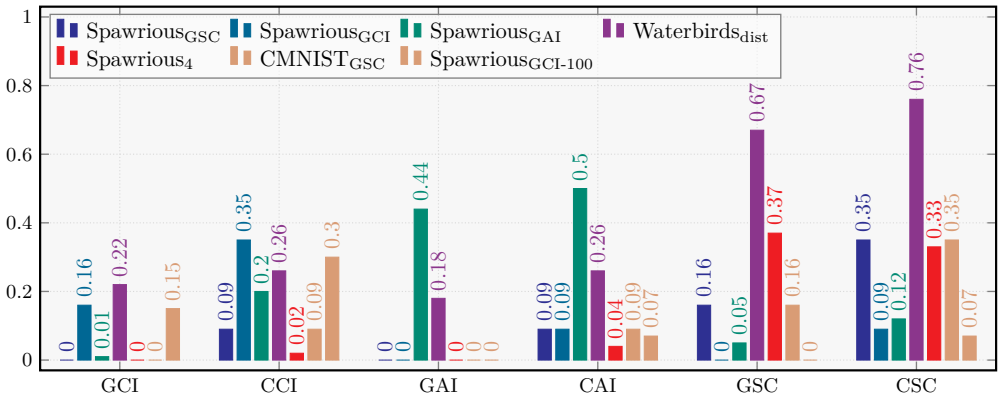

Figure 3: Global and Client statistical data heterogeneity metrics of each of the proposed datasets. Note how each dataset has different values of class imbalance, attribute imbalance and spurious correlations both globally and in the clients.

1. Probabilistic Selection (SC): The first criterion for selecting a client is based on the presence of spurious correlations. The probability distribution p_{SC} over all clients, based on the SC dimension of the data heterogeneity triplet (DHT) $\tilde{\Delta}^k$ is given by: $p_{\text{SC}} = \frac{\tilde{\Delta}_3}{\|\tilde{\Delta}_3\|_1}, \quad p_{\text{SC}} \in [0,1]^K$, where $\tilde{\Delta}_3$ is a vector composed of the SC values of all clients. The probability of selecting each client is proportional to its corresponding value in p_{SC}.

2. Complementary Selection (AI or CI): After selecting a client based on SC, the next step ensures that the next selected client exhibits complementary data heterogeneity. To do so, the server computes the row-normalized matrix $\underline{\tilde{\Delta}}$, where $\underline{\tilde{\Delta}}_i^k = \frac{\tilde{\Delta}_i^k}{\sum_{i=1}^{3} \tilde{\Delta}_i^k}, \quad \forall i \in \{1,2,3\}, \forall k \in \mathcal{K}$. Using $\underline{\tilde{\Delta}}$, the server selects the client whose normalized triplet is the least aligned (i.e. has the smallest dot product) with the normalized triplet of the already selected client. Formally, this is computed as: $k_c = \arg\min_{k \in \mathcal{K} \setminus \{k_p\}} \left\langle \underline{\tilde{\Delta}}^{k_p}, \underline{\tilde{\Delta}}^{k} \right\rangle$ where k_p denotes the already selected client and $\langle \cdot, \cdot \rangle$ represents the dot product.

3. Orthogonal Selection (CI or AI): The next client k_r is chosen to complement the heterogeneity profile of the data of the clients already selected. To achieve this, the server selects the client whose DHT aligns the most with the vector perpendicular to the DHTs of the two previously selected clients (which represent SC and either CI or AI). Formally, this is computed as: $k_r = \arg\max_{k \in \mathcal{K} \setminus \{k_p, k_c\}} \left\langle \underline{\tilde{\Delta}}^{k_p} \times \underline{\tilde{\Delta}}^{k_c}, \underline{\tilde{\Delta}}^{k} \right\rangle$ where $(\cdot \times \cdot)$ is the cross product, ensuring that the selected client exhibits heterogeneity in the remaining dimension.

This client selection approach leverages all three dimensions of the DHT by selecting clients with different types of data heterogeneity. The server repeats the steps above iteratively until the desired number of clients has been selected, excluding clients already chosen in the current round. To enhance variability, the order in which dimensions (SC, CI, AI) are prioritized is rotated every three clients.

As illustrated in the experimental section, FedDiverse's client selection can be applied in conjunction with any FL optimization approach.

5 Experiments

5.1 Datasets

We perform the experimental evaluation taking as a basis three computer vision datasets that are commonly used for benchmarking algorithms in the presence of statistical data heterogeneity. From these three base datasets, we create 7 different datasets that cover a wide variety of CI, AI and SC both globally and in the clients, as explained next and reflected in Fig. 3.

Table 1: Worst group accuracies (mean and std) over three experiments of FedDiverse and the baselines in a federation with 24 to 100 clients, with 9 clients selected every round, and FedAvgM as the FL optimization algorithm. The best-performing method is highlighted with **bold**, and the second best is underlined. (*): 12 clients selected from 100. (**): Not scalable due to excessive computational cost.

Client Selection algorithm	Dataset						
	$\text{Spawrious}_{\text{GSC}}$	$\text{Spawrious}_{\text{GCI}}$	$\text{Spawrious}_{\text{GAI}}$	$\text{WaterBirds}_{\text{dist}}$	Spawrious_4	$\text{CMNIST}_{\text{GSC}}$	$\text{Spawrious}_{\text{GCI-100}}$*
FedDiverse	88.01 ± 0.96	**89.91** ± 1.91	**87.28** ± 1.61	54.10 ± 2.03	**86.06** ± 0.58	**94.01** ± 0.98	**91.22** ± 1.61
Uniform random	86.27 ± 1.12	87.59 ± 2.00	85.86 ± 2.56	42.42 ± 0.59	84.02 ± 0.63	92.00 ± 1.61	86.96 ± 1.28
Round robin	87.12 ± 0.87	87.64 ± 0.90	86.17 ± 2.65	41.23 ± 2.18	83.54 ± 1.83	93.51 ± 0.49	85.54 ± 0.40
FedNova	87.49 ± 0.73	88.52 ± 1.49	87.22 ± 0.47	42.83 ± 0.71	84.65 ± 0.64	93.23 ± 0.34	87.33 ± 0.18
pow-d	**89.12** ± 0.32	89.01 ± 1.18	86.91 ± 1.52	**56.75** ± 2.49	83.54 ± 2.01	92.85 ± 0.47	89.85 ± 1.00
FedPNS	85.75 ± 1.34	85.02 ± 9.12	82.22 ± 6.94	48.75 ± 12.14	84.35 ± 1.45	91.49 ± 1.42	N/A**
HCSFed	86.80 ± 0.86	87.17 ± 0.27	85.96 ± 2.70	41.66 ± 1.80	85.59 ± 0.66	91.45 ± 1.11	85.49 ± 0.78

WaterBirds The WaterBirds dataset [WBW+11] is an image classification dataset with two classes (*waterbirds* and *landbirds*), and two background attributes (*water* and *land*). In the training set, there is a spurious correlation where waterbirds are more often found on water backgrounds, and landbirds are more often seen on land backgrounds. We follow the original train/test split and distribute the training data over 30 clients as follows: 3 clients predominantly have CI; 2 clients have mostly AI; and the rest of the clients are impacted largely by the same SC as the global dataset.

Spawrious The Spawrious dataset [LDKS23] consists of 4 dog breeds (target labels y) on 6 background (attributes a) groups generated with Stable Diffusion v1.4 [RBL+22]. There are 6,336 images for each (y, a) pair, making it the largest vision dataset where the level of spurious correlation is adjustable [YZC+24]. We save 10% of the data to create a balanced test set and use the remaining data to generate 5 federated datasets with various levels of statistical data heterogeneity. We identify and use the 2 hardest background groups (namely *beach* and *snow*) together with 2 (*labrador* and *dachshund*) or 4 (*labrador*, *dachshund*, *bulldog*, and *corgi*) dog breed classes.

While the WaterBirds dataset contains CI, AI and SC (see Fig. 3), we create 5 Spawrious datasets with different data distributions to investigate the impact of CI, AI and SC individually:

First, we create 3 datasets where only one type of data heterogeneity is present globally: spurious correlation in Spawrious_{GSC}; class imbalance in Spawrious_{GCI}; and attribute imbalance in Spawrious_{GAI}. Second, we create Spawrious_4 which contains high levels of spurious correlation and 4 classes. Third, we create $\text{Spawrious}_{\text{GCI-100}}$ with class imbalance and 100 clients.

CMNIST The CMNIST dataset [ABGL19] is generated based on the binarized MNIST dataset, with labels $y = 0$ for digits less than five and $y = 1$ otherwise. The attribute is given by the foreground color, $\mathcal{A} = \{\text{red}, \text{green}\}$. We use the same data distribution as for Spawrious_{GSC} with 2 classes. Hence, in this dataset there is a high level of global and client spurious correlations.

5.2 Experimental Setup

We simulate a federated learning scenario with a total of 24 to 100 clients depending on the dataset[4] on a machine with 3 Nvidia A100-80G GPUs using both the Flower [BTM+20] and PyTorch [PGM+19] frameworks. Our code is available in *anonymized for blind revision*.

The server and the clients trained a MobileNet v2 [How17] model, where batch normalization layers were replaced with group normalization layers and initial weights are pre-trained on Imagenet. We applied the *categorical crossentropy* loss function with 0.001 learning rate and a batch size of 28. Unless otherwise noted, we used $T = 200$ rounds of federated training with equally weighted clients. In experiments without client selection, all clients (24 to 100) participate in the federation in every round. In the cases where client

[4]The federations with the Spawrious_{GSC}, Spawrious_{GCI} and CMNIST_{GSC} datasets have 24 clients; Spawrious_{GAI} and Spawrious_4 have 25 clients; WaterBirds_{dist} has 30 clients; and $\text{Spawrious}_{GCI-100}$ has 100 clients.

selection is performed, the server selects 9 clients to participate in the federation in each round, except for $\text{Spawrious}_{\text{GCI-100}}$ where 12 clients are selected.

We performed all experiments on the previously described datasets. We report *worst-group accuracy* [SKHL20] and its standard deviation, defined as $\min_{(y,a)\in\mathcal{Y}\times\mathcal{A}} \mathbb{E}[\mathbb{1}\{y = f(x;\theta)\} \mid Y = y, A = a]$ over 3 runs using a balanced global test dataset.

5.3 Baselines

We compare FedDiverse's client selection strategy with 6 baselines, described below. All the methods are implemented using server side momentum FedAvgM [HQB19].

1. Uniform random selection, where clients are randomly selected according to a uniform distribution.

2. Round robin selection, where the server keeps track of how many times R_k a client k has been selected such that the client cannot participate again while $\exists j \neq k, R_j < R_k$.

3. FedNova [WLL+20], a client weighting approach by means of importance weighting. The parameter aggregation is given by $\theta^{t+1} = \theta^t - \tau_{eff} \sum_k \frac{|D_k|}{|D|} \cdot \beta \nabla_k^{t+1}$, where β is the same momentum as in FedAvgM and τ_{eff} is the effective iteration step and it is computed from the client's steps.

4. pow-d [CWJ22], a loss-based selection method. First, the server $\mathcal{S}$ selects $k_{br} : \kappa < \kappa_{br} < K$ clients randomly to broadcast the model parameters θ^t. All $k \in S_{\kappa_{br}}$ clients compute $\ell(\theta^t, D_k)$ and report it back to the server. Then, the server sorts the clients such that for $i, j \in \{1, \ldots, K\}, i < j \rightarrow \ell(\theta^t, D_i) < \ell(\theta^t, D_j)$ and selects the first κ clients to participate in the computation of θ^{t+1}.

5. FedPNS [WW22] identifies clients that negatively impact the aggregated gradient change by comparing a client's gradient change ∇_k^{t+1} with the overall gradient change excluding that client, $\nabla^{t+1} - \nabla_k^{t+1}$. If a client slows down the aggregated gradient, as indicated by $\langle \nabla^{t+1}, (\nabla^{t+1} - \nabla_k^{t+1}) \rangle$, the client is flagged. Flagged clients are less likely to be selected in subsequent rounds, while non-flagged clients and those not sampled in round t are more likely to be selected.

6. HCSFed [SSG+23] clusters the clients based on the compressed gradients after the first round of training. We use 3 clusters and randomly select clients from each cluster.

5.4 Communication and Computation Overhead

The baselines have varying levels of communication and computation overhead reported in Table 2. FedNova performs client weighting instead of selection, hence, all the clients participate in the federation in each round. While pow-d performs client selection, the server needs $\ell(\theta^t, D_k)$ from all clients to determine which clients to select in each round. FedPNS requires no additional work from the clients, but the server calculates the similarity between the client gradient updates in every round, which can result in significant overhead for complex models and large number of clients. HCSFed addresses this issue by compressing the model gradients and organizing the clients into clusters after the first training round and minimizing the overhead for subsequent rounds. Uniform random, Round robin and FedDiverse are the only three client selection methods where **only the participating clients** perform computations and communicate with the server in each round. FedDiverse's additional communication overhead is limited to just 3 scalar values per client while the client-side computational overhead occurs only in a single training round. The only recurring overhead is the server-side selection, which involves sorting clients based on their DHT values.

5.5 Results

Tab. 1 depicts the worst group accuracies for FedDiverse and all the baselines on the 7 datasets. Note how client selection with FedDiverse is the *only method* that yields competitive performance across all datasets.

Table 2: Communication and computation overhead for FedDiverse and the baselines where $K = 24..100, r = 10^{-5}, |\theta| = 2.23 \cdot 10^6, n_k = 10^2..10^3$

Method	Frequency	Communication Overhead	Computation Overhead Client	Computation Overhead Server ($\forall t$)
FedDiverse	$t = 1$	3	$\forall k \in \mathcal{K} : 2O(n_k\|\theta\|)$	$O(K)$
Round Robin	0	0	0	$O(1)$
FedNova	$\forall t$	$3 + \forall k \notin \mathcal{K} : \theta_k^t$	$O(1) + \forall k \notin \mathcal{K} : O(n_k\|\theta\|)$	$O(K)$
pow-d	$\forall t$	$1 + \forall k \notin \mathcal{K} : \theta_k$	$\forall k \notin \mathcal{K} : O(n_k\|\theta\|)$	$O(K \log K)$
FedPNS	0	0	0	$O(K^2\|\theta\|^2)$
HCSFed	$t = 1$	$r\theta_k$	$r\|\theta\|^2$	$t = 1 : O(K \cdot r\|\theta\|)$ $t \neq 1 : O(K)$

Table 3: Worst group accuracies (mean and std) over three experiments of FedDiverse combined with four FL optimization methods on the proposed datasets vs the default random selection. The best-performing client selection method is highlighted in bold and the best-performing combination is underlined. Note how all the FL optimization algorithms improve their performance when doing client selection with FedDiverse vs random selection across all datasets.

FL algorithm	$\text{Spawrious}_{\text{GSC}}$		$\text{Spawrious}_{\text{GCI}}$		$\text{Spawrious}_{\text{GAI}}$		$\text{WaterBirds}_{\text{dist}}$		Spawrious_{4}		$\text{CMNIST}_{\text{GSC}}$	
	Random	FedDiverse	Random	FedDiverse	Random	FedDiverse	Random	FedDiverse	Random	FedDiverse	Random	FedDiverse
FedAvg	85.09 ± 1.00	**85.90** ± 1.62	85.65 ± 3.85	**89.43** ± 0.63	80.49 ± 0.52	**84.33** ± 1.51	31.72 ± 3.05	**46.47** ± 1.31	81.07 ± 1.29	**83.86** ± 1.20	87.58 ± 2.38	**91.01** ± 0.58
FedAvgM	86.27 ± 1.12	**88.01** ± 0.96	87.59 ± 2.00	**89.91** ± 1.91	85.86 ± 2.56	**87.28** ± 1.61	42.42 ± 0.59	**54.10** ± 2.03	**84.02** ± 0.63	**86.06** ± 0.58	92.00 ± 1.61	**94.01** ± 0.98
FedProx	84.43 ± 1.91	**86.33** ± 1.49	82.91 ± 4.89	**87.30** ± 3.01	81.39 ± 2.12	**83.81** ± 2.46	31.57 ± 2.87	**43.51** ± 0.70	80.44 ± 1.55	**83.64** ± 0.74	91.36 ± 0.95	**91.49** ± 1.86
FedAvgM + FedProx	85.41 ± 1.67	**87.85** ± 1.26	88.38 ± 1.42	**90.48** ± 1.61	**85.65** ± 3.76	85.17 ± 1.79	44.29 ± 1.26	**53.84** ± 0.90	82.97 ± 0.69	**86.12** ± 0.97	92.42 ± 0.71	**93.24** ± 0.38

5.6 Benchmarking FedDiverse with FL methods

We evaluate FedDiverse's ability to improve the robustness of existing FL optimization algorithms when combined with them. We aim to (1) evaluate the ability of FedDiverse's client selection method to improve performance across a variety of datasets and FL optimization algorithms; and (2) shed light on which method yields the best performance. The algorithms benchmarked in this section are:

1. FedAvg [MMR+17], which serves as the baseline FL method where in each round the global model is replaced by the average of the client models.

2. FedAvgM [HQB19], which includes server-level momentum, inspired by the momentum algorithm [Nes13]. It is designed to improve non-IID convergence. The momentum parameter is set to $\beta = 0.95$.

3. FedProx [LSTS20], where the client loss contains a proximal term derived from the difference between server and client weights to stabilize the convergence: $\ell_{prox}(f_k(x;\theta_k), y) = \ell(f_k(x;\theta_k), y) + \frac{\mu}{2}||\theta - \theta_k||_2$, where μ is a parameter set to 0.1 in our experiments.

As FedAvgM changes the server aggregation method, FedProx the local loss function, and FedDiverse the client selection policy, we can use any combination of the 3 methods to mitigate statistical data heterogeneity. As reflected in Tab. 3, FedDiverse improves the performance over random selection when combined with every FL method and in all datasets. The combination of FedDiverse with FedAvgM yields very competitive performance and hence we opt for FedAvgM as the FL optimization method to be used in all of the experiments.

5.7 Ablation study

In this section, we study the performance of FedDiverse on the WaterBirds dataset and under different configurations, reflected in Tab. 4. We compare 3 scenarios:

1. Our realistic setup, where the interaction matrix $\tilde{N}^k$ and the data heterogeneity triplets $\tilde{\Delta}^k$ are estimated;

2. An ideal –yet unrealistic– scenario where the interaction matrix N^k and therefore the triplets Δ^k are known to the server; and

3. A method where the full interaction matrix N^k is sent to the server instead of the triplets. In this case, the server first computes the client weights ω_k that minimize the variance of the matrix $\mathbf{S} = \sum_{k \in \mathcal{K}} \omega_k N^k$, *i.e.*, $\min \mathrm{Var}(\mathbf{S}) = \frac{1}{|Y||A|} \sum_{y \in Y} \sum_{a \in A} (s_{y,a} - \nu)^2$, where ν is the average number of samples per (y, a) groups. We solve it as a convex optimization problem and use the ω_k weight as the probability to sample client k. Note that this method would raise privacy concerns.

Furthermore, we evaluate the impact of increasing the number of pre-training steps and compare FedDiverse when combined with FedAvg and FedAvgM.

As seen in the table, perfect knowledge of N^k could yield an increase of up to 5.71 and 3.74 points in worst group accuracy with FedAvg and FedAvgM, respectively. Communicating the true (typically unknown) interaction matrix instead of the triplets could add up to 4.15 and 4.78 points to the worst-group accuracy with FedAvg and FedAvgM, respectively. Increasing the number of pre-training steps is only helpful with FedAvgM, yet the performance gains are not significant.

Table 4: Ablation study of FedDiverse with different configurations on the WaterBirds dataset.

Pre-training (T_0)	**Interaction matrix**	**Message**	**Worst group accuracy (%)** FedAvg	FedAvgM
20	predicted	DHT($\tilde{\Delta}^k$)	44.03 ± 0.32	55.04 ± 3.09
1	predicted	DHT($\tilde{\Delta}^k$)	46.47 ± 1.31	54.10 ± 2.03
20	known	DHT(Δ^k)	48.08 ± 3.27	58.00 ± 0.77
1	known	DHT(Δ^k)	50.62 ± 3.00	58.88 ± 2.57
20	known	N^k	49.74 ± 2.30	58.41 ± 2.04
1	known	N^k	51.82 ± 3.79	57.84 ± 0.48

6 Conclusion

In this work, we have introduced a novel framework for characterizing statistical data heterogeneity in FL, we have presented seven datasets to evaluate the performance of FL methods in the presence of different types of data heterogeneity, and we have proposed FedDiverse, a novel and efficient client selection method that selects clients with diverse types of statistical data heterogeneity. In extensive experiments, we demonstrate FedDiverse's competitive performance on all datasets while requiring low communication and computation overhead.

Acknowledgment

This research was funded by the European Union. Views and opinions expressed are however those of the author(s) only and do not necessarily reflect those of the European Union or the European Health and Digital Executive Agency (HaDEA). Neither the European Union nor the granting authority can be held responsible for them. G.D.N. and N.O. have been partially supported by funding received at the ELLIS Unit Alicante Foundation by the European Commission under the Horizon Europe Programme - Grant Agreement 101120237 - ELIAS, and a nominal grant from the Regional Government of Valencia in Spain (Convenio Singular signed with Generalitat Valenciana, Conselleria de Innovación, Industria, Comercio y Turismo, Dirección General de Innovación). G.D.N. is also funded by a grant by the Banco Sabadell Foundation. G.D.N., E.F., Y.J.N., and N.Q. have been supported in part by the European Research Council under the European Union's Horizon 2020 research and innovation programme Grant Agreement no. 851538 - BayesianGDPR. N.Q. has been supported in part by the Horizon Europe research and innovation programme Grant Agreement no. 101120763 - TANGO. N.Q. is also supported by BCAM Severo Ochoa accreditation CEX2021-001142-S/MICIN/AEI/10.13039/501100011033.

References

[ABGL19] M. Arjovsky, L. Bottou, I. Gulrajani, and D. Lopez-Paz, "Invariant risk minimization," *arXiv preprint arXiv:1907.02893*, 2019 (cit. on pp. 3, 9).

[AZM+21] D. A. E. Acar, Y. Zhao, R. Matas, M. Mattina, P. Whatmough, and V. Saligrama, "Federated learning based on dynamic regularization," in *International Conference on Learning Representations*, 2021. [Online]. Available: https://openreview.net/forum?id=B7v4QMR6Z9w (cit. on pp. 2, 3).

[BCM+18] T. S. Brisimi, R. Chen, T. Mela, A. Olshevsky, I. C. Paschalidis, and W. Shi, "Federated learning of predictive models from federated electronic health records," *International journal of medical informatics*, vol. 112, pp. 59–67, 2018 (cit. on p. 2).

[BEGS17] P. Blanchard, E. M. El Mhamdi, R. Guerraoui, and J. Stainer, "Machine learning with adversaries: Byzantine tolerant gradient descent," *Advances in neural information processing systems*, vol. 30, 2017 (cit. on p. 4).

[BTM+20] D. J. Beutel, T. Topal, A. Mathur, X. Qiu, J. Fernandez-Marques, Y. Gao, L. Sani, H. L. Kwing, T. Parcollet, P. P. d. Gusmão, and N. D. Lane, "Flower: A friendly federated learning research framework," *arXiv preprint arXiv:2007.14390*, 2020 (cit. on p. 9).

[CCC22] D. Caldarola, B. Caputo, and M. Ciccone, "Improving generalization in federated learning by seeking flat minima," in *European Conference on Computer Vision*, Springer, 2022, pp. 654–672 (cit. on p. 2).

[CGSY18] T. Chen, G. Giannakis, T. Sun, and W. Yin, "Lag: Lazily aggregated gradient for communication-efficient distributed learning," *Advances in neural information processing systems*, vol. 31, 2018 (cit. on p. 4).

[CKMT18] S. Caldas, J. Konečny, H. B. McMahan, and A. Talwalkar, "Expanding the reach of federated learning by reducing client resource requirements," *arXiv preprint arXiv:1812.07210*, 2018 (cit. on p. 4).

[CV25] H. Chen and H. Vikalo, "Heterogeneity-guided client sampling: Towards fast and efficient non-iid federated learning," *Advances in Neural Information Processing Systems*, vol. 37, pp. 65 525–65 561, 2025 (cit. on p. 4).

[CWJ22] Y. J. Cho, J. Wang, and G. Joshi, "Towards understanding biased client selection in federated learning," in *International Conference on Artificial Intelligence and Statistics*, PMLR, 2022, pp. 10 351–10 375 (cit. on pp. 3, 4, 10).

[CWKM20] Y. Chen, C. Wei, A. Kumar, and T. Ma, "Self-training avoids using spurious features under domain shift," in *Proceedings of the 34th International Conference on Neural Information Processing Systems*, ser. NIPS '20, Vancouver, BC, Canada: Curran Associates Inc., 2020, ISBN: 9781713829546 (cit. on p. 2).

[CYZ19] C. Clark, M. Yatskar, and L. Zettlemoyer, "Don't take the easy way out: Ensemble based methods for avoiding known dataset biases," in *Proceedings of the 2019 Conference on Empirical Methods in Natural Language Processing and the 9th International Joint Conference on Natural Language Processing (EMNLP-IJCNLP)*, K. Inui, J. Jiang, V. Ng, and X. Wan, Eds., Hong Kong, China: Association for Computational Linguistics, Nov. 2019, pp. 4069–4082. DOI: 10.18653/v1/D19-1418. [Online]. Available: https://aclanthology.org/D19-1418 (cit. on p. 3).

[DLS21] D. K. Dennis, T. Li, and V. Smith, "Heterogeneity for the win: One-shot federated clustering," in *International Conference on Machine Learning*, PMLR, 2021, pp. 2611–2620 (cit. on p. 4).

[DZC+23] J. Dong, D. Zhang, Y. Cong, W. Cong, H. Ding, and D. Dai, "Federated incremental semantic segmentation," in *Proceedings of the IEEE/CVF Conference on Computer Vision and Pattern Recognition*, 2023, pp. 3934–3943 (cit. on p. 21).

[FCC23] E. Fanì, M. Ciccone, and B. Caputo, "Feddrive v2: An analysis of the impact of label skewness in federated semantic segmentation for autonomous driving," in *5th Italian Conference on Robotics and Intelligent Machines (I-RIM)*, 2023 (cit. on p. 21).

[FMO20] A. Fallah, A. Mokhtari, and A. Ozdaglar, "Personalized federated learning with theoretical guarantees: A model-agnostic meta-learning approach," *Advances in neural information processing systems*, vol. 33, pp. 3557–3568, 2020 (cit. on p. 2).

[GJM+20] R. Geirhos, J.-H. Jacobsen, C. Michaelis, R. Zemel, W. Brendel, M. Bethge, and F. A. Wichmann, "Shortcut learning in deep neural networks," *Nature Machine Intelligence*, vol. 2, no. 11, pp. 665–673, 2020 (cit. on pp. 2, 3).

[GTL23] Y. Guo, X. Tang, and T. Lin, "Fedrc: Tackling diverse distribution shifts challenge in federated learning by robust clustering," *arXiv preprint arXiv:2301.12379*, 2023 (cit. on pp. 4, 7).

[How17] A. G. Howard, "Mobilenets: Efficient convolutional neural networks for mobile vision applications," *arXiv preprint arXiv:1704.04861*, 2017 (cit. on p. 9).

[HQB19] T.-M. H. Hsu, H. Qi, and M. Brown, "Measuring the effects of non-identical data distribution for federated visual classification," *arXiv preprint arXiv:1909.06335*, 2019 (cit. on pp. 3, 10, 11, 18).

[HSF+23] H. Huang, W. Shi, Y. Feng, C. Niu, G. Cheng, J. Huang, and Z. Liu, "Active client selection for clustered federated learning," *IEEE Transactions on Neural Networks and Learning Systems*, 2023 (cit. on pp. 4, 7).

[HZRS16] K. He, X. Zhang, S. Ren, and J. Sun, "Deep residual learning for image recognition," in *Proceedings of the IEEE conference on computer vision and pattern recognition*, 2016, pp. 770–778 (cit. on p. 18).

[KHL19] D. Kaushik, E. Hovy, and Z. C. Lipton, "Learning the difference that makes a difference with counterfactually-augmented data," *arXiv preprint arXiv:1909.12434*, 2019 (cit. on p. 3).

[KJK+20] S. P. Karimireddy, M. Jaggi, S. Kale, M. Mohri, S. J. Reddi, S. U. Stich, and A. T. Suresh, "Mime: Mimicking centralized stochastic algorithms in federated learning," *arXiv preprint arXiv:2008.03606*, 2020 (cit. on p. 3).

[KKK+19] B. Kim, H. Kim, K. Kim, S. Kim, and J. Kim, "Learning not to learn: Training deep neural networks with biased data," in *Proceedings of the IEEE/CVF conference on computer vision and pattern recognition*, 2019, pp. 9012–9020 (cit. on p. 3).

[KKM+20] S. P. Karimireddy, S. Kale, M. Mohri, S. Reddi, S. Stich, and A. T. Suresh, "Scaffold: Stochastic controlled averaging for federated learning," in *International conference on machine learning*, PMLR, 2020, pp. 5132–5143 (cit. on pp. 2, 3).

[KMA+21] P. Kairouz, H. B. McMahan, B. Avent, A. Bellet, M. Bennis, A. N. Bhagoji, K. Bonawitz, Z. Charles, G. Cormode, R. Cummings, *et al.*, "Advances and open problems in federated learning," *Foundations and trends® in machine learning*, vol. 14, no. 1–2, pp. 1–210, 2021 (cit. on pp. 2, 3).

[LDKS23] A. Lynch, G. J.-S. Dovonon, J. Kaddour, and R. Silva, *Spawrious: A benchmark for fine control of spurious correlation biases*, 2023. arXiv: `2303.05470 [cs.CV]` (cit. on p. 9).

[LHC+21] E. Z. Liu, B. Haghgoo, A. S. Chen, A. Raghunathan, P. W. Koh, S. Sagawa, P. Liang, and C. Finn, "Just train twice: Improving group robustness without training group information," in *International Conference on Machine Learning*, PMLR, 2021, pp. 6781–6792 (cit. on pp. 2, 3).

[LHS21] Q. Li, B. He, and D. Song, "Model-contrastive federated learning," in *Proceedings of the IEEE/CVF conference on computer vision and pattern recognition*, 2021, pp. 10 713–10 722 (cit. on p. 3).

[LHY+20] X. Li, K. Huang, W. Yang, S. Wang, and Z. Zhang, "On the convergence of fedavg on non-iid data," *International Conference on Learning Representations*, 2020 (cit. on p. 2).

[LSTS20] T. Li, A. K. Sahu, A. Talwalkar, and V. Smith, "Federated learning: Challenges, methods, and future directions," *IEEE signal processing magazine*, vol. 37, no. 3, pp. 50–60, 2020 (cit. on pp. 1–3, 11, 18).

[MBB24] A. Mora, A. Bujari, and P. Bellavista, "Enhancing generalization in federated learning with heterogeneous data: A comparative literature review," *Future Generation Computer Systems*, 2024 (cit. on pp. 2, 3).

[MMR+17] B. McMahan, E. Moore, D. Ramage, S. Hampson, and B. A. y Arcas, "Communication-efficient learning of deep networks from decentralized data," in *Artificial intelligence and statistics*, PMLR, 2017, pp. 1273–1282 (cit. on pp. 1, 5, 11).

[NAN20] V. Nagarajan, A. Andreassen, and B. Neyshabur, "Understanding the failure modes of out-of-distribution generalization," *arXiv preprint arXiv:2010.15775*, 2020 (cit. on p. 3).

[NCA+20] J. Nam, H. Cha, S. Ahn, J. Lee, and J. Shin, "Learning from failure: De-biasing classifier from biased classifier," *Advances in Neural Information Processing Systems*, vol. 33, pp. 20 673–20 684, 2020 (cit. on pp. 3, 7, 21).

[Nes13] Y. Nesterov, "Gradient methods for minimizing composite functions," *Mathematical programming*, vol. 140, no. 1, pp. 125–161, 2013 (cit. on p. 11).

[NLQO22] G. D. Németh, M. A. Lozano, N. Quadrianto, and N. M. Oliver, "A snapshot of the frontiers of client selection in federated learning," *Transactions on Machine Learning Research*, 2022, ISSN: 2835-8856. [Online]. Available: `https://openreview.net/forum?id=vwOKBldzFu` (cit. on p. 4).

[PGM+19] A. Paszke, S. Gross, F. Massa, A. Lerer, J. Bradbury, G. Chanan, T. Killeen, Z. Lin, N. Gimelshein, L. Antiga, A. Desmaison, A. Kopf, E. Yang, Z. DeVito, M. Raison, A. Tejani, S. Chilamkurthy, B. Steiner, L. Fang, J. Bai, and S. Chintala, "Pytorch: An imperative style, high-performance deep learning library," in *Advances in Neural Information Processing Systems 32*, Curran Associates, Inc., 2019, pp. 8024–8035. [Online]. Available: `http://papers.neurips.cc/paper/9015-pytorch-an-imperative-style-high-performance-deep-learning-library.pdf` (cit. on pp. 9, 21).

[PLY23] P. Pene, W. Liao, and W. Yu, "Incentive design for heterogeneous client selection: A robust federated learning approach," *IEEE Internet of Things Journal*, vol. 11, no. 4, pp. 5939–5950, 2023 (cit. on pp. 4, 7).

[RBL+22] R. Rombach, A. Blattmann, D. Lorenz, P. Esser, and B. Ommer, "High-resolution image synthesis with latent diffusion models," in *Proceedings of the IEEE/CVF conference on computer vision and pattern recognition*, 2022, pp. 10 684–10 695 (cit. on p. 9).

[RCZ+20] S. Reddi, Z. Charles, M. Zaheer, Z. Garrett, K. Rush, J. Konečnỳ, S. Kumar, and H. B. McMahan, "Adaptive federated optimization," *arXiv preprint arXiv:2003.00295*, 2020 (cit. on p. 3).

[RMLH22] N. Rodríguez-Barroso, E. Martínez-Cámara, M. V. Luzón, and F. Herrera, "Dynamic defense against byzantine poisoning attacks in federated learning," *Future Generation Computer Systems*, vol. 133, pp. 1–9, 2022 (cit. on p. 4).

[SFT+23] D. Shenaj, E. Fanì, M. Toldo, D. Caldarola, A. Tavera, U. Michieli, M. Ciccone, P. Zanuttigh, and B. Caputo, "Learning across domains and devices: Style-driven source-free domain adaptation in clustered federated learning," in *Proceedings of the IEEE/CVF winter conference on applications of computer vision*, 2023, pp. 444–454 (cit. on p. 21).

[SKHL20] S. Sagawa, P. W. Koh, T. B. Hashimoto, and P. Liang, "Distributionally Robust Neural Networks for Group Shifts: On the Importance of Regularization for Worst-Case Generalization," in *International Conference on Learning Representations*, 2020. arXiv: `1911.08731` (cit. on pp. 3, 10).

[SSG+23] D. Song, G. Shen, D. Gao, L. Yang, X. Zhou, S. Pan, W. Lou, and F. Zhou, "Fast heterogeneous federated learning with hybrid client selection," in *Uncertainty in Artificial Intelligence*, PMLR, 2023, pp. 2006–2015 (cit. on pp. 4, 10).

[STW19] T. Song, Y. Tong, and S. Wei, "Profit allocation for federated learning," in *2019 IEEE International Conference on Big Data (Big Data)*, IEEE, 2019, pp. 2577–2586 (cit. on p. 4).

[TCK+21] F. Träuble, E. Creager, N. Kilbertus, F. Locatello, A. Dittadi, A. Goyal, B. Schölkopf, and S. Bauer, "On disentangled representations learned from correlated data," in *Proceedings of the 38th International Conference on Machine Learning*, M. Meila and T. Zhang, Eds., ser. Proceedings of Machine Learning Research, vol. 139, PMLR, Jul. 2021, pp. 10 401–10 412 (cit. on p. 2).

[TYCY22] A. Z. Tan, H. Yu, L. Cui, and Q. Yang, "Towards personalized federated learning," *IEEE transactions on neural networks and learning systems*, vol. 34, no. 12, pp. 9587–9603, 2022 (cit. on p. 2).

[WBW+11] C. Wah, S. Branson, P. Welinder, P. Perona, and S. Belongie, "The caltech-ucsd birds-200-2011 dataset," 2011 (cit. on p. 9).

[WFK+24] Y. Wang, H. Fu, R. Kanagavelu, Q. Wei, Y. Liu, and R. S. M. Goh, "An aggregation-free federated learning for tackling data heterogeneity," in *Proceedings of the IEEE/CVF Conference on Computer Vision and Pattern Recognition*, 2024, pp. 26 233–26 242 (cit. on p. 3).

[WLL+20] J. Wang, Q. Liu, H. Liang, G. Joshi, and H. V. Poor, "Tackling the objective inconsistency problem in heterogeneous federated optimization," *Advances in neural information processing systems*, vol. 33, pp. 7611–7623, 2020 (cit. on pp. 4, 10).

[WSK+22] J. Wolfrath, N. Sreekumar, D. Kumar, Y. Wang, and A. Chandra, "Haccs: Heterogeneity-aware clustered client selection for accelerated federated learning," in *2022 IEEE international parallel and distributed processing symposium (IPDPS)*, IEEE, 2022, pp. 985–995 (cit. on p. 4).

[WW22] H. Wu and P. Wang, "Node selection toward faster convergence for federated learning on non-iid data," *IEEE Transactions on Network Science and Engineering*, vol. 9, no. 5, pp. 3099–3111, 2022 (cit. on pp. 4, 10).

[WZNK24] X. Wang, H. Zhao, K. Nahrstedt, and S. Koyejo, "Personalized federated learning with spurious features: An adversarial approach," *Transactions on Machine Learning Research*, 2024 (cit. on pp. 3, 21).

[WZY+19] T. Wang, J. Zhao, M. Yatskar, K.-W. Chang, and V. Ordonez, "Balanced datasets are not enough: Estimating and mitigating gender bias in deep image representations," in *Proceedings of the IEEE/CVF international conference on computer vision*, 2019, pp. 5310–5319 (cit. on p. 3).

[XZLD22] F. Xin, J. Zhang, J. Luo, and F. Dong, "Federated learning client selection mechanism under system and data heterogeneity," in *2022 IEEE 25th International Conference on Computer Supported Cooperative Work in Design (CSCWD)*, IEEE, 2022, pp. 1239–1244 (cit. on p. 4).

[YAE+18] T. Yang, G. Andrew, H. Eichner, H. Sun, W. Li, N. Kong, D. Ramage, and F. Beaufays, "Applied federated learning: Improving google keyboard query suggestions," *arXiv preprint arXiv:1812.02903*, 2018 (cit. on p. 2).

[YGQ+22] C.-H. Yao, B. Gong, H. Qi, Y. Cui, Y. Zhu, and M.-H. Yang, "Federated multi-target domain adaptation," in *Proceedings of the IEEE/CVF Winter Conference on Applications of Computer Vision*, 2022, pp. 1424–1433 (cit. on p. 21).

[YLCT20] E. Yurtsever, J. Lambert, A. Carballo, and K. Takeda, "A survey of autonomous driving: Common practices and emerging technologies," *IEEE access*, vol. 8, pp. 58 443–58 469, 2020 (cit. on p. 2).

[YNX+23] R. Ye, Z. Ni, C. Xu, J. Wang, S. Chen, and Y. C. Eldar, "Fedfm: Anchor-based feature matching for data heterogeneity in federated learning," *IEEE Transactions on Signal Processing*, vol. 71, pp. 4224–4239, 2023 (cit. on p. 3).

[YWL+22] H. Yao, Y. Wang, S. Li, L. Zhang, W. Liang, J. Zou, and C. Finn, "Improving Out-of-Distribution Robustness via Selective Augmentation," in *Proceedings of the 39th International Conference on Machine Learning*, ser. Proceedings of Machine Learning Research, vol. 162, PMLR, Jul. 2022, pp. 25 407–25 437 (cit. on p. 3).

[YZC+24] W. Ye, G. Zheng, X. Cao, Y. Ma, and A. Zhang, "Spurious correlations in machine learning: A survey," *arXiv preprint arXiv:2402.12715*, 2024 (cit. on pp. 2, 3, 9).

[YZKG23] Y. Yang, H. Zhang, D. Katabi, and M. Ghassemi, "Change is hard: A closer look at subpopulation shift," in *International Conference on Machine Learning*, PMLR, 2023, pp. 39 584–39 622 (cit. on pp. 2, 5, 7, 18).

[ZFH21] P. Zhou, P. Fang, and P. Hui, "Loss tolerant federated learning," *arXiv preprint arXiv:2105.03591*, 2021 (cit. on p. 4).

[ZLT+23] J. Zhang, A. Li, M. Tang, J. Sun, X. Chen, F. Zhang, C. Chen, Y. Chen, and H. Li, "Fed-cbs: A heterogeneity-aware client sampling mechanism for federated learning via class-imbalance reduction," in *International Conference on Machine Learning*, PMLR, 2023, pp. 41 354–41 381 (cit. on pp. 4, 7).

[ZS18] Z. Zhang and M. Sabuncu, "Generalized cross entropy loss for training deep neural networks with noisy labels," *Advances in neural information processing systems*, vol. 31, 2018 (cit. on pp. 7, 21).

[ZWL+24] J. Zhang, J. Wang, Y. Li, F. Xin, F. Dong, J. Luo, and Z. Wu, "Addressing heterogeneity in federated learning with client selection via submodular optimization," *ACM Transactions on Sensor Networks*, vol. 20, no. 2, pp. 1–32, 2024 (cit. on p. 3).

[ZZWC20] R. Zeng, S. Zhang, J. Wang, and X. Chu, "Fmore: An incentive scheme of multi-dimensional auction for federated learning in mec," in *2020 IEEE 40th international conference on distributed computing systems (ICDCS)*, IEEE, 2020, pp. 278–288 (cit. on p. 4).

A Additional details on the FL datasets

In this section, we include additional details on the proposed FL datasets. To construct each dataset, we first define the global interaction matrix (given for WaterBirds) such that a centralized ERM training has at least 3.2% drop between worst group and average accuracy. This ensures that the statistical data heterogeneity will have impact on the training. Table 5 summarizes the results on the centralized version of the datasets.

Table 5: Details of the global data distributions of the datasets. Performance measured by training MobileNetV2 for 10 epochs with SGD

Dataset	(1) $\text{Spawrious}_{\text{GSC}}$, (2) $\text{CMNIST}_{\text{GSC}}$	$\text{Spawrious}_{\text{GCI}}$	$\text{Spawrious}_{\text{GAI}}$	$\text{WaterBirds}_{\text{dist}}$	Spawrious_4
Interaction Matrix (N)	$\begin{bmatrix} 1760 & 640 \\ 640 & 1760 \end{bmatrix}$	$\begin{bmatrix} 1760 & 1760 \\ 640 & 640 \end{bmatrix}$	$\begin{bmatrix} 2000 & 500 \\ 2000 & 100 \end{bmatrix}$	$\begin{bmatrix} 3498 & 184 \\ 56 & 1057 \end{bmatrix}$	$\begin{bmatrix} 2000 & 200 \\ 2000 & 200 \\ 200 & 2000 \\ 200 & 2000 \end{bmatrix}$
Average accuracy (%)	(1) 93.15, (2) 96.35	92.92	93.9	82.37	93.07
Worst group accuracy(%)	(1) 87.82, (2) 93.15	87.62	89.09	55.09	85.88
Class Imbalance (CI)	0	0.16	0.01	0.22	0
Attribute Imbalance (AI)	0	0	0.44	0.18	0
Spurious Correlation (SC)	0.16	0	0.05	0.67	0.37

In Table 6, we show the data distribution between clients. Each cell of the table shows a type of client: $m \times N^k, \Delta^k$, where m is the number of clients of that type, N^k is the interaction matrix of that type of client and Δ^k is the data heterogeneity triplet (DHT) of that type. Note that the different datasets are designed for federations with different numbers of clients such that the overall imbalance in the dataset size among clients remains small.

B Comparison with different architectures

In Table 7, we report experiments with ResNet50 [HZRS16] on the WaterBirds dataset. Note that computer vision models used in FL scenarios are typically smaller than a ResNet50 [HQB19; LSTS20]. However, the spurious correlation literature in centralized machine learning uses this model in the reported benchmarks [YZKG23]. Thus, we include this experiment for completeness. As we can observe, FedDiverse improves the performance also on the ResNet50.

C Pre-training with a different number of rounds

In Table 8 we summarize the experimental results obtained when increasing the number of pre-training rounds before using the FedDiverse algorithm to determine the values of the clients' DHTs. Note how using $T_0 = 1$ yields similar results than using more pre-training rounds (with full participation). Thus, we keep $T_0 = 1$ in all experiments to reduce the computation and communication costs.

D Sensitivity analysis of the hyper-parameters of the FedDiverse algorithm

To determine the right hyper-parameters for FedDiverse, we conducted an experiment on the $\text{Spawrious}_{\text{GSC}}$ dataset by changing the following 3 hyper-parameters: the training steps of the *biased model* $\tau_{biased} = \{5, 25, 50, 75, 100\}$, the training steps of the *attribute classifier* $\tau_{attr} = \{5, 25, 50, 75, 100\}$, and the q value of the *generalized cross-entropy loss* $q = \{0.1, 0.3, 0.5, 0.7, 0.9\}$. We performed an exhaustive grid search on these values. Figure 4 summarizes the results of this sensitivity analysis. We report the Euclidean distance between the predicted and true DHT values, thus the best parameters correspond to the smallest distance

$$\min_{\tau_{biased}, \tau_{attr}, q} \operatorname*{avg}_{k \in 1..K} ||\tilde{\Delta}^k - \Delta^k||$$

In conclusion, we use $\tau_{biased} = 50$, $\tau_{attr} = 10$, and select $q = 0.3$ as the best q value for the given τ parameters.

Table 6: Client interaction matrices and ground-truth triplets for the proposed FL data distributions. Each cell of the table contains a client interaction matrix in the middle, the number of clients with that matrix on the left, and the CI, AI, and SC values of the matrix on the right.

Spawrious$_{\text{GSC}}$, CMNIST$_{\text{GSC}}$	$\Delta^{\text{CI}}_{\text{AI}}$ SC	**Spawrious$_{\text{GCI}}$**	$\Delta^{\text{CI}}_{\text{AI}}$ SC	**Spawrious$_{\text{GAI}}$**	$\Delta^{\text{CI}}_{\text{AI}}$ SC	**WaterBirds$_{\text{dist}}$**	$\Delta^{\text{CI}}_{\text{AI}}$ SC	**Spawrious$_4$**	$\Delta^{\text{CI}}_{\text{AI}}$ SC	**Spawrious$_{\text{GCI-100}}$**	$\Delta^{\text{CI}}_{\text{AI}}$ SC
$2 \times \begin{bmatrix} 90 & 90 \\ 10 & 10 \end{bmatrix}$	0.53 0.00 0.00	$15 \times \begin{bmatrix} 90 & 90 \\ 10 & 10 \end{bmatrix}$	0.53 0.00 0.00	$1 \times \begin{bmatrix} 120 & 5 \\ 20 & 10 \end{bmatrix}$	0.29 0.54 0.15	$1 \times \begin{bmatrix} 23 & 23 \\ 10 & 110 \end{bmatrix}$	0.15 0.28 0.18	$2 \times \begin{bmatrix} 20 & 20 \\ 20 & 20 \\ 5 & 5 \\ 5 & 5 \end{bmatrix}$	0.14 0.00 0.00	$64 \times \begin{bmatrix} 68 & 68 \\ 10 & 10 \end{bmatrix}$	0.45 0.00 0.00
$2 \times \begin{bmatrix} 10 & 10 \\ 90 & 90 \end{bmatrix}$	0.53 0.00 0.00	$1 \times \begin{bmatrix} 10 & 10 \\ 90 & 90 \end{bmatrix}$	0.53 0.00 0.00	$1 \times \begin{bmatrix} 120 & 40 \\ 5 & 10 \end{bmatrix}$	0.58 0.14 0.07	$1 \times \begin{bmatrix} 110 & 23 \\ 10 & 23 \end{bmatrix}$	0.28 0.15 0.18	$2 \times \begin{bmatrix} 5 & 5 \\ 5 & 5 \\ 20 & 20 \\ 20 & 20 \end{bmatrix}$	0.14 0.00 0.00	$4 \times \begin{bmatrix} 10 & 10 \\ 68 & 68 \end{bmatrix}$	0.45 0.00 0.00
$2 \times \begin{bmatrix} 90 & 10 \\ 90 & 10 \end{bmatrix}$	0.00 0.53 0.00	$2 \times \begin{bmatrix} 90 & 10 \\ 90 & 10 \end{bmatrix}$	0.00 0.53 0.00	$2 \times \begin{bmatrix} 170 & 5 \\ 5 & 5 \end{bmatrix}$	0.70 0.70 0.24	$1 \times \begin{bmatrix} 89 & 39 \\ 1 & 29 \end{bmatrix}$	0.30 0.01 0.27	$2 \times \begin{bmatrix} 20 & 5 \\ 20 & 5 \\ 20 & 5 \\ 20 & 5 \end{bmatrix}$	0.00 0.28 0.00	$8 \times \begin{bmatrix} 68 & 10 \\ 68 & 10 \end{bmatrix}$	0.00 0.45 0.00
$2 \times \begin{bmatrix} 10 & 90 \\ 10 & 90 \end{bmatrix}$	0.00 0.53 0.00	$2 \times \begin{bmatrix} 10 & 90 \\ 10 & 90 \end{bmatrix}$	0.00 0.53 0.00	$2 \times \begin{bmatrix} 5 & 5 \\ 170 & 5 \end{bmatrix}$	0.70 0.70 0.24	$1 \times \begin{bmatrix} 29 & 39 \\ 1 & 89 \end{bmatrix}$	0.01 0.30 0.27	$2 \times \begin{bmatrix} 5 & 20 \\ 5 & 20 \\ 5 & 20 \\ 5 & 20 \end{bmatrix}$	0.00 0.28 0.00	$8 \times \begin{bmatrix} 10 & 68 \\ 10 & 68 \end{bmatrix}$	0.00 0.45 0.00
$15 \times \begin{bmatrix} 90 & 10 \\ 10 & 90 \end{bmatrix}$	0.00 0.00 0.53	$2 \times \begin{bmatrix} 90 & 10 \\ 10 & 90 \end{bmatrix}$	0.00 0.00 0.53	$2 \times \begin{bmatrix} 10 & 30 \\ 120 & 10 \end{bmatrix}$	0.21 0.21 0.38	$1 \times \begin{bmatrix} 81 & 35 \\ 9 & 31 \end{bmatrix}$	0.18 0.02 0.14	$1 \times \begin{bmatrix} 5 & 20 \\ 5 & 20 \\ 20 & 5 \\ 20 & 5 \end{bmatrix}$	0.00 0.00 0.19	$8 \times \begin{bmatrix} 68 & 10 \\ 10 & 68 \end{bmatrix}$	0.00 0.00 0.45
$1 \times \begin{bmatrix} 10 & 90 \\ 90 & 10 \end{bmatrix}$	0.00 0.00 0.53	$2 \times \begin{bmatrix} 10 & 90 \\ 90 & 10 \end{bmatrix}$	0.00 0.00 0.53	$2 \times \begin{bmatrix} 80 & 80 \\ 20 & 2 \end{bmatrix}$	0.47 0.01 0.08	$9 \times \begin{bmatrix} 126 & 1 \\ 1 & 31 \end{bmatrix}$	0.28 0.28 0.87	$7 \times \begin{bmatrix} 119 & 5 \\ 119 & 5 \\ 5 & 119 \\ 5 & 119 \end{bmatrix}$	0.00 0.00 0.50	$8 \times \begin{bmatrix} 10 & 68 \\ 68 & 10 \end{bmatrix}$	0.00 0.00 0.45
				$14 \times \begin{bmatrix} 80 & 15 \\ 90 & 2 \end{bmatrix}$	0.00 0.56 0.06	$16 \times \begin{bmatrix} 127 & 1 \\ 1 & 31 \end{bmatrix}$	0.28 0.28 0.87	$9 \times \begin{bmatrix} 118 & 5 \\ 118 & 5 \\ 5 & 118 \\ 5 & 118 \end{bmatrix}$	0.00 0.00 0.50		
				$1 \times \begin{bmatrix} 110 & 5 \\ 85 & 8 \end{bmatrix}$	0.01 0.66 0.01						

Table 7: Study of FedDiverse combined with other non-IID mitigation techniques using different machine learning models on the Waterbirds$_{\text{dist}}$ dataset.

FL algorithm	**MobileNet**		**ResNet50**	
	Random	FedDiverse	Random	FedDiverse
FedAvg	31.72 ± 3.05	**46.47** ± 1.31	59.97 ± 2.47	**65.47** ± 2.31
FedAvgM	42.42 ± 0.59	**54.10** ± 2.03	62.56 ± 0.78	**67.81** ± 2.87
FedProx	31.57 ± 2.87	**43.51** ± 0.70	62.36 ± 0.94	**69.11** ± 1.92
FedAvgM + FedProx	44.29 ± 1.26	**53.84** ± 0.90	64.54 ± 3.29	**66.77** ± 4.16

Table 8: Study on the effect of pre-training rounds on the final worst group accuracy and determining the DHT values of the FedDiverse algorithm in WaterBirds$_{\text{dist}}$ dataset using FedAvg and FedAvgM algorithms for server-side aggregation.

Pre-training(T_0)	**Worst group accuracy(%)**		**DHT prediction error $\|\|\tilde{\Delta}^k - \Delta^k\|\|$**	
	FedAvg	FedAvgM	FedAvg	FedAvgM
1	**46.47** ± 1.31	54.10 ± 2.03	0.50 ± 0.03	0.50 ± 0.10
5	42.47 ± 1.56	52.80 ± 2.45	0.49 ± 0.07	0.54 ± 0.01
10	42.16 ± 4.29	51.97 ± 4.43	**0.47** ± 0.01	0.52 ± 0.02
15	41.20 ± 3.73	53.12 ± 4.54	**0.47** ± 0.06	0.52 ± 0.05
20	<u>44.03</u> ± 0.32	**55.04** ± 3.09	<u>0.48</u> ± 0.02	<u>0.49</u> ± 0.01
30	42.16 ± 2.39	<u>54.36</u> ± 2.45	0.49 ± 0.02	**0.47** ± 0.04

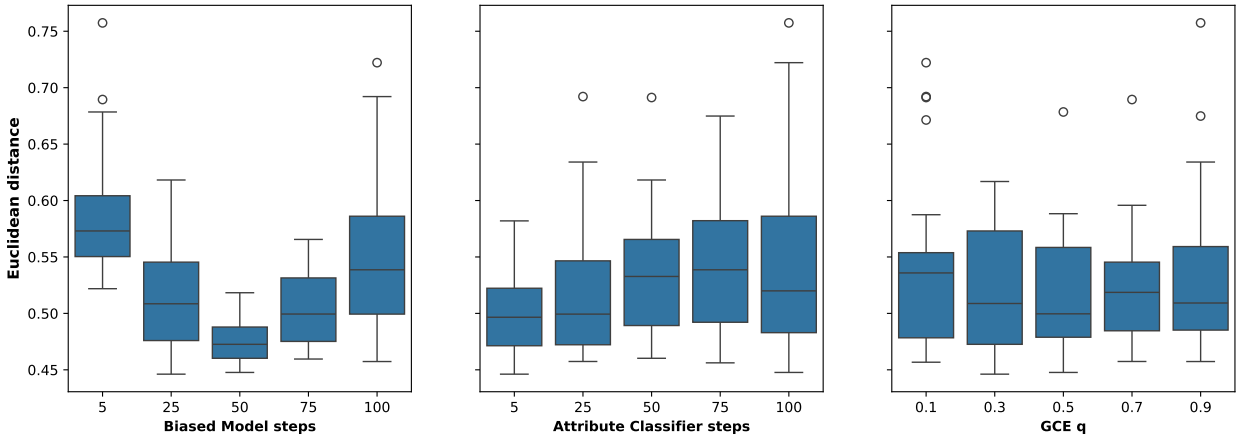

Figure 4: FedDiverse's sensitivity to the biased model's training steps τ_{biased}, the attribute classifier training steps τ_{attr} and the generalized cross-entropy loss' q value (q). We use $\tau_{biased} = 50$, $\tau_{attr} = 10$, and selected $q = 0.3$ as best q value for the given τ parameters.

E FedDiverse pseudo-code

Algorithm 6 contains the pseudo-code of the FedDiverse algorithm. Specifically:

- Algorithm 1 contains the pseudo-code for FedDiverse's pre-training phase.
- Algorithm 2 shows how clients in FedDiverse train the biased model.
- Algorithm 3 corresponds to how clients in FedDiverse train the attribute classifier.
- Algorithm 4 illustrates how FedDiverse computes the data heterogeneity triplets.
- Algorithm 5 contains FedDiverse's sampling strategy according to the data heterogeneity triplets.
- Algorithm 6 depicts the overall procedure.

F Analysis of FedDiverse's sampling strategy

Figures 5 to 9 show the distribution of clients sampled per round as per the FedDiverse client selection algorithm (as specifically described in Algorithms 5 and 6) on the $\text{Spawrious}_{\text{GSC}}$, $\text{Spawrious}_{\text{GCI}}$, $\text{Spawrious}_{\text{GAI}}$, Spawrious_{4} and $\text{WaterBirds}_{\text{dist}}$ datasets, respectively. Note that the simulation conducted on Figure 5 can equivalently be considered as for the $\text{CMNIST}_{\text{GSC}}$ dataset, since both $\text{CMNIST}_{\text{GSC}}$ and $\text{Spawrious}_{\text{GSC}}$ have the same clients distributions.

The figures are based on a simulation where 9 clients are sampled per round over 20 training rounds, following the setup described in the main paper. Each client is assigned a type –CI, AI, or SC– based on the highest values of their corresponding metrics, as detailed in Table 6. Clients are then sorted by type, with CI clients having lowest IDs, followed by AI and SC clients. The background color in the figures represents the client type while the percentage in the background indicates the average selection rate for that type across all 20 rounds. In this simulation, we assume that the server has full knowledge of the clients' true data heterogeneity triplets.

These plots illustrate how FedDiverse samples the clients in a much more uniform way within each type, as the percentages are close to 33.3%. Interestingly, Figure 9 shows that the 3 clients of type CI are sampled in each round, proving how FedDiverse effectively succeeds in sampling clients with different types of data heterogeneity.

G Generalization for multiclass problems

In this section, we further discuss the generalization of the interaction matrix predictor for multiclass problems. Following [NCA+20], we train a biased classifier to identify the strongest correlation with a binary attribute present in the dataset. They used the generalized cross-entropy loss ℓ_{CE}, introduced in [ZS18] as:

$$\ell_{GCE}(p(x;\theta), y) = \frac{1 - p_y(x;\theta)^q}{q}, \tag{11}$$

where, for $\lim_{q\to 0} \frac{1-p^q}{q} = -\log p$ we get the standard binary cross-entropy

$$\ell_{BCE}(p(x;\theta), y) = -(y \log p(x;\theta) + (1-y)\log(1 - p(x;\theta))). \tag{12}$$

In their experiments, [NCA+20] successfully used ℓ_{GCE} to amplify the bias for binary classification problems. However, given that Pytorch [PGM+19] implements multiclass classification as

$$\ell_{CCE}(p(x;\theta), y) = \frac{1}{|M|} \sum_{p \in M} -\log\left(\frac{e^{p_y(x,\theta)}}{\sum_{j\in Y} e^{p_j(x,\theta)}}\right), \tag{13}$$

where M is the set of positive classes the sample, we chose to keep the biased classifier binary. This means that instead of a multiclass classification problem, we train $|Y|$ binary classification models ($\bar{f}_k^b$) such that for the $b \in Y$ selected class

$$y^* = \begin{cases} 1, & \text{if } y = b \\ 0, & \text{otherwise} \end{cases} \tag{14}$$

We construct the $\tilde{G}_k$ and $\tilde{g}_k$ class-by-class: if the binary classifier $\bar{f}_k^b$ classified the sample from class b correctly, it counts for the majority ($\tilde{G}$), otherwise the minority ($\tilde{g}$).

H Limitations and future work

To the best of our knowledge, FedDiverse is the first algorithm specifically designed to address the issue of spurious correlations in Federated Learning. As noted by [WZNK24], the heterogeneity among clients can help mitigate learning shortcuts that arise from these spurious correlations. Unlike their approach, which leverages spurious features to create a Personalized FL solution, the goal of FedDiverse is to develop a single global model that is resilient to spurious correlations. Furthermore, FedDiverse leverages various types of statistical data heterogeneity in the clients during each sampling round to enhance the generalization capabilities of the model and reduce the overall impact of data heterogeneity.

However, FedDiverse is not exempt from limitations. First, it has been designed and evaluated specifically for image classification tasks. In future work, we plan to extend FedDiverse to other computer vision tasks, such as semantic segmentation for FL, a topic of growing interest in the community [DZC+23; YGQ+22; SFT+23; FCC23]. The presence of spuriously correlated features in these tasks could pose security risks by leading models to rely on misleading patterns, potentially compromising their performance in safety-critical applications.

Furthermore, FedDiverse could be improved by addressing scenarios with multiple spurious attributes, each with more than two possible values. Future versions could be designed to approximate multi-dimensional interaction tensors rather than the current bi-dimensional interaction matrices N_k. These tensors would link the true ground-truth label with various spurious attributes, accommodating more complex attribute interactions.

Algorithm 1 - Pre-training(κ, T_0, τ_0)

Let: Model f, global parameters θ^0
for each round $t \in [T_0]$ **do**
  Randomly sample $\mathcal{K}' \subseteq \mathcal{K}$ such that $|\mathcal{K}'| = \kappa$
  $\mathcal{S}$ sends global parameters θ^t to all the clients in $\mathcal{K}'$
  for each client $k \in \mathcal{K}'$, *in parallel* **do**
    $\theta_k = \theta^t$
    $\theta_k^{t+1} = \text{ERM}(f(\theta_k); \ell_{\text{CE}}; D_k; \tau_0)$
    Send θ_k^{t+1} to $\mathcal{S}$
  end for
  $\theta^{t+1} = \sum_{k \in \mathcal{K}'} \frac{n_k}{n} \theta_k^{t+1}$
end for
Return θ^{T_0}

Algorithm 2 - Biased-model-training(θ^{T_0}, τ_{bias}, q)

Let: $\ell_{\text{GCE}}(\bar{f}_k(x;\theta), y) = \frac{1-\bar{f}_k(x;\theta)^q}{q}$
Initialize parameters θ_k of the biased model $\bar{f}_k$ with pre-trained parameters θ^{T_0}
$\theta_k^{\text{bias}} = \text{ERM}(\bar{f}_k(\theta_k); \ell_{\text{GCE}}; D_k; \tau_{\text{bias}})$
$\tilde{G}_k$ = set of inputs x such that the samples $(x, y) \in D_k$ are correctly predicted by $\bar{f}_k$, *i.e.* $\bar{f}_k(x; \theta_k^{\text{bias}}) = y$
$\tilde{g}_k$ = set of inputs x such that the samples $(x, y) \in D_k$ are incorrectly predicted by $\bar{f}_k$, *i.e.* $\bar{f}_k(x; \theta_k^{\text{bias}}) \neq y$

Return θ_k^{bias}, $\tilde{G}_k$, $\tilde{g}_k$

Algorithm 3 - Attribute-classifier-training($\tilde{G}^k$, $\tilde{g}^k$, θ_k^{bias}, τ_{attr})

Let: $\hat{f} = \hat{\psi} \circ \varphi$; $\hat{\psi}$ is the attribute classifier, φ is the feature extractor
Compute the pivot class $\hat{y} = \arg\min_{y \in \mathcal{Y}} \left| |\tilde{G}_y^k| - |\tilde{g}_y^k| \right|$
Construct the dataset $\hat{D}_k$ of pairs $(x, \tilde{a})$, for all x such that $(x, \hat{y}) \in D_k$. $\tilde{a} = 0$ if $x \in G_{\hat{y}}^k$, $\tilde{a} = 1$ otherwise
Initialize parameters $\theta_k = \theta_k^{\text{bias}}$
Fix the parameters of the feature extractor φ
$\theta_k^{\text{attr}} = \text{ERM}(\hat{f}(\theta_k); \ell_{\text{CE}}; D_k; \tau_{\text{attr}})$
Return θ_k^{attr}, $\hat{y}$

Algorithm 4 - DHT-computation($\hat{y}$, $\tilde{G}_{\hat{y}}^k$, $\tilde{g}_{\hat{y}}^k$)

Let: $D_k^y \subset D_k$ is the set of images in D_k with label y
$\tilde{N} = 0_{|\mathcal{Y}| \times 2}$
for each $y \in \mathcal{Y}$: **do**
  if $y = \hat{y}$ **then**
    $\tilde{N}_{y0} = |\tilde{G}_{\hat{y}}^k|$, $\tilde{N}_{y1} = |\tilde{g}_{\hat{y}}^k|$
  else
    for each $(x, y) \in D_k^y$ **do**
      $\tilde{a} = \hat{f}(x; \theta_k^{\text{attr}})$
      $\tilde{N}_{y\tilde{a}} = \tilde{N}_{y\tilde{a}} + 1$
    end for
  end if
end for
$\tilde{\Delta}^k = [\Delta_{\text{CI}}(\tilde{N}^k), \Delta_{\text{AI}}(\tilde{N}^k), \Delta_{\text{SC}}(\tilde{N}^k)]^\top$
Return $\tilde{\Delta}^k$

Algorithm 5 - Triplet-sampling($\tilde{\Delta}$, $\mathcal{K}_{\text{left}}$, i)

1) Probabilistic selection

Compute the probability vector $p = \frac{\tilde{\Delta}_i}{\left\|\tilde{\Delta}_i\right\|_1}$

Sample $k_p \in \mathcal{K}_{\text{left}}$ according to p

Remove k_p from $\mathcal{K}_{\text{left}}$: $\mathcal{K}_{\text{left}} = \mathcal{K}_{\text{left}} \setminus \{k_p\}$

2) Complementary selection

Compute the normalized matrix $\underline{\tilde{\Delta}}$ such that $\underline{\tilde{\Delta}}^k = \frac{\tilde{\Delta}^k}{\left\|\tilde{\Delta}^k\right\|_1}$, $\forall k \in \mathcal{K}$

Find the complementary client $k_c = \arg\min_{k \in \mathcal{K}_{\text{left}}} \left\langle \underline{\tilde{\Delta}}^{k_p}, \underline{\tilde{\Delta}}^k \right\rangle$

Remove k_c from $\mathcal{K}_{\text{left}}$: $\mathcal{K}_{\text{left}} = \mathcal{K}_{\text{left}} \setminus \{k_c\}$

3) Orthogonal selection

Find the remaining orthogonal client $k_r = \arg\max_{k \in \mathcal{K} \setminus \{k_p, k_c\}} \left\langle \underline{\tilde{\Delta}}^{k_p} \times \underline{\tilde{\Delta}}^{k_c}, \underline{\tilde{\Delta}}^k \right\rangle$

Remove k_r from $\mathcal{K}_{\text{left}}$: $\mathcal{K}_{\text{left}} = \mathcal{K}_{\text{left}} \setminus \{k_r\}$

Return k_p, k_c, k_r, $\mathcal{K}_{\text{left}}$

Algorithm 6 - FedDiverse algorithm. Here, we assume that $\kappa \mod 3 \equiv 0$ for readability. If $\kappa \mod 3 \not\equiv 0$, the last time Algorithm 5 is executed in one round, it will return fewer clients accordingly.

Input: Number of clients sampled per round κ, number of pre-training rounds T_0, number of training rounds T, number of steps of local training τ_0, number of steps of local biased model training τ_{bias}, number of steps of local attribute classifier training τ_{attr}, ℓ_{GCE} hyper-parameter $q \in (0, 1]$, FL optimization algorithm Opt, FL aggregator Agg

$\tilde{\Delta} = 0_{3 \times K}$

θ^{T_0} = Pre-training(κ, T_0, τ_0)

$\mathcal{S}$ sends θ^{T_0} to all the clients $k \in \mathcal{K}$

for each client $k \in \mathcal{K}$ *in parallel* **do**

  θ_k^{bias}, $\tilde{G}^k$, $\tilde{g}^k$ = Biased-model-training(θ^{T_0}, τ_{bias}, q)

  θ_k^{attr}, $\hat{y}$ = Attribute-classifier-training($\tilde{G}^k$, $\tilde{g}^k$, θ_k^{bias}, τ_{attr})

  $\tilde{\Delta}^k$ = DHT-computation($\hat{y}$, $\tilde{G}_{\hat{y}}^k$, $\tilde{g}_{\hat{y}}^k$)

end for

for each round $t \in [T]$ **do**

  $\mathcal{K}_{\text{left}} = \mathcal{K}$

  $\mathcal{K}' = \emptyset$

  while $|\mathcal{K}'| < \kappa$ **do**

    k_p, k_c, k_r, $\mathcal{K}_{\text{left}}$ = Triplet-sampling($\tilde{\Delta}$, $\mathcal{K}_{\text{left}}$, $t \mod 3$)

    $\mathcal{K}' = \mathcal{K}' \cup \{k_p, k_c, k_r\}$

  end while

  $\mathcal{S}$ sends global parameters θ^t (and, eventually, additional information) to all the clients in $\mathcal{K}'$

  for each client $k \in \mathcal{K}'$ *in parallel* **do**

    θ_k^{t+1}, ... = Opt(θ^t, ...) # Specific parameters and returned values depend on the chosen Opt algorithm

    Send θ_k^{t+1} and eventual other information to $\mathcal{S}$ # Specific message depends on the chosen Opt algorithm

  end for

  θ^{t+1}, ... =Agg($\{\theta_k^{t+1}\}_{k \in \mathcal{K}'}$, ...) # Specific parameters and returned values depend on the chosen Agg algorithm

end for

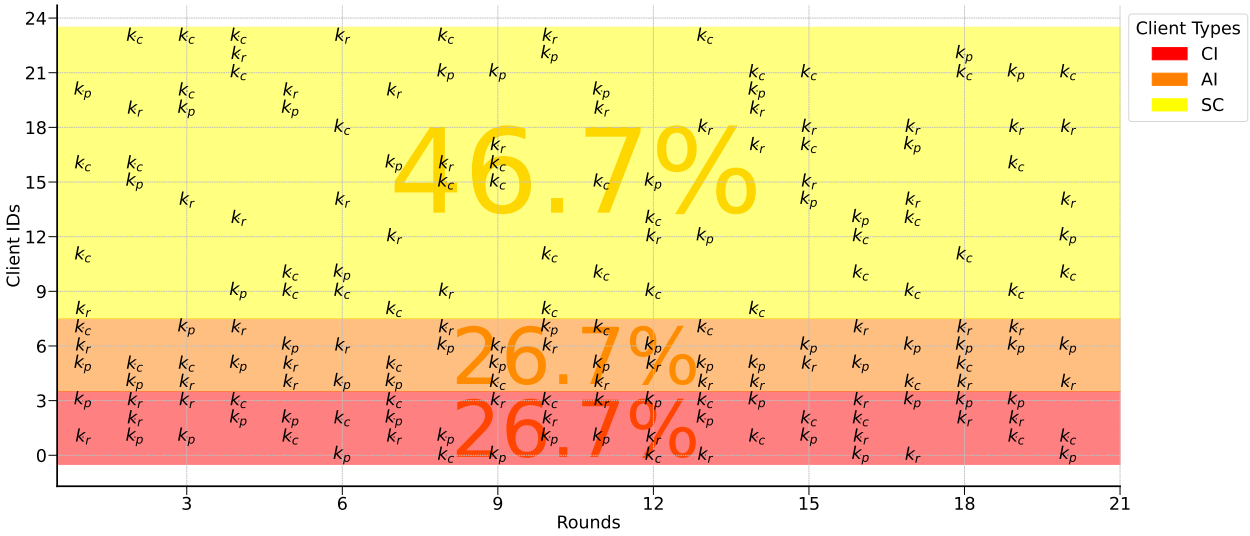

Figure 5: Simulation of the sampling strategy of FedDiverse on the $\text{Spawrious}_{\text{GSC}}$ dataset. With uniform random sampling, clients belonging to each specific type would have been sampled with the following proportions: CI=16.7%, AI=16.7%, SC=66.6%. This simulation can be equivalently interpreted as if the dataset is $\text{CMNIST}_{\text{GSC}}$ since the two datasets have the same client distributions.

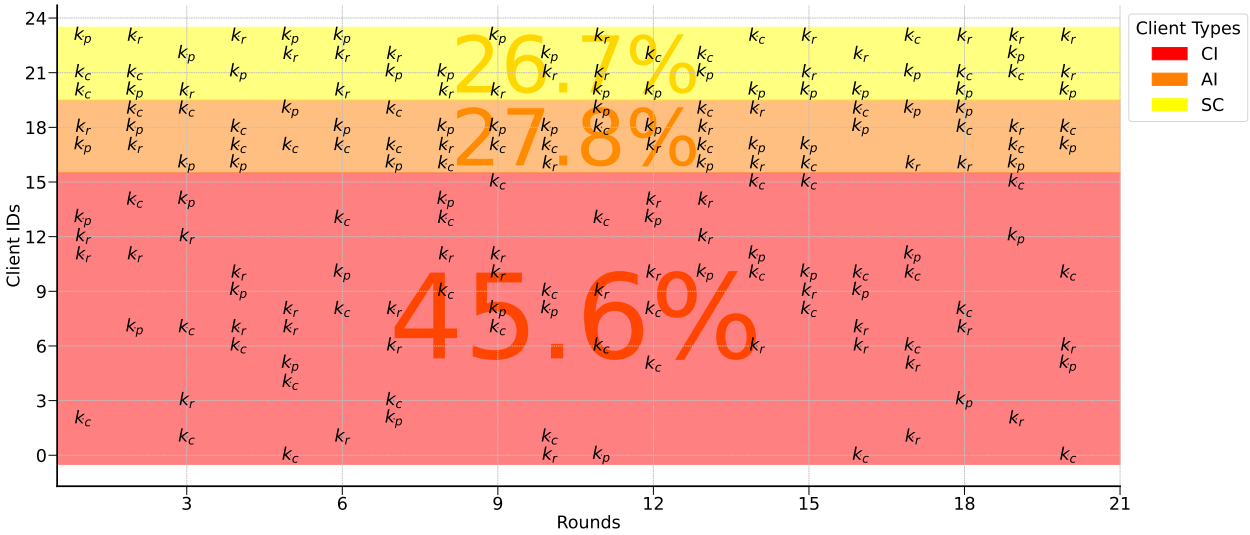

Figure 6: Simulation of the sampling strategy of FedDiverse on the $\text{Spawrious}_{\text{GCI}}$ dataset. With uniform random sampling, clients belonging to each specific type would have been sampled with the following proportions: CI=66.6%, AI=16.7%, SC=16.7%.

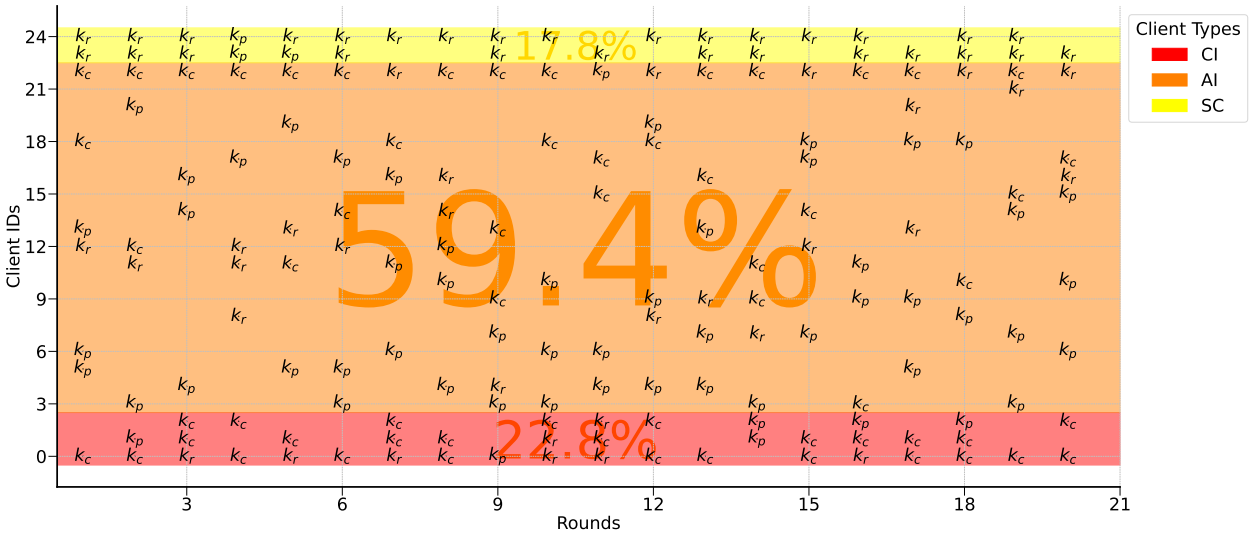

Figure 7: Simulation of the sampling strategy of FedDiverse on the $\text{Spawrious}_{\text{GAI}}$ dataset. With uniform random sampling, clients belonging to each specific type would have been sampled with the following proportions: CI=12.0%, AI=60.0%, SC=8.0%.

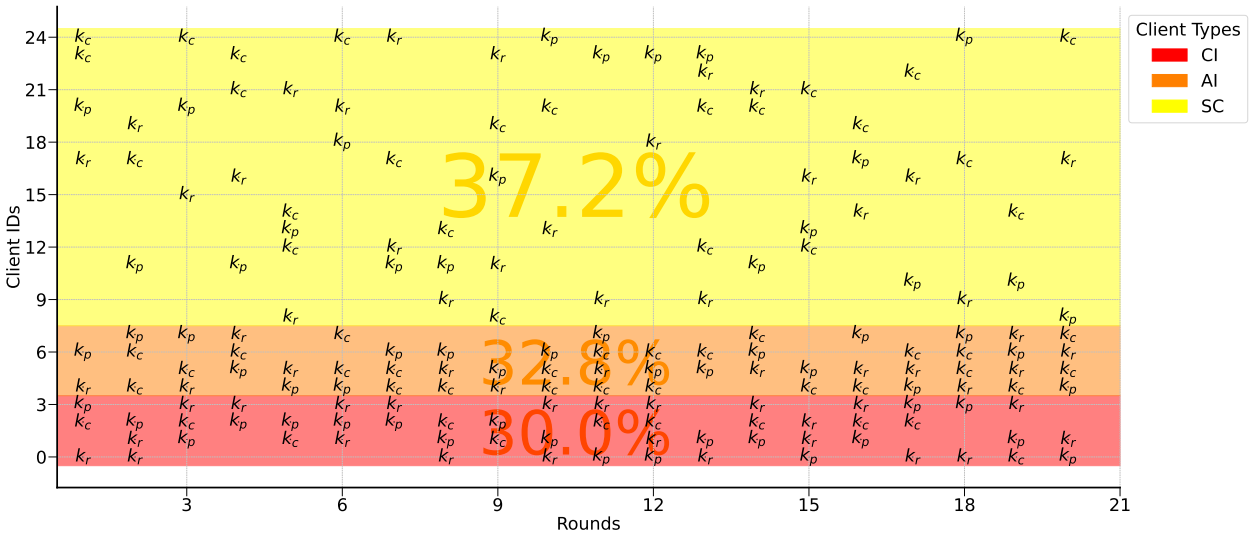

Figure 8: Simulation of the sampling strategy of FedDiverse on the Spawrious_4 dataset. With uniform random sampling, clients belonging to each specific type would have been sampled with the following proportions: CI=16.0%, AI=16.0%, SC=68.0%.

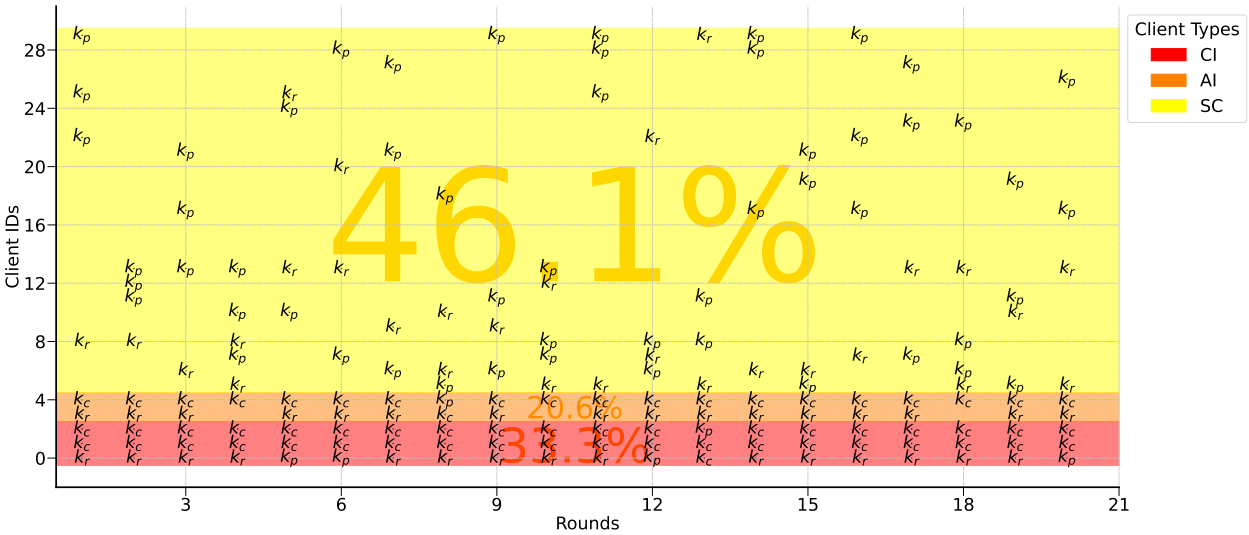

Figure 9: Simulation of the sampling strategy of FedDiverse on the $\text{Waterbirds}_{\text{dist}}$ dataset. With uniform random sampling, clients belonging to each specific type would have been sampled with the following proportions: CI=10.0%, AI=6.7%, SC=83.3%.